The DOE Program in High Energy Density Physics:
New Initiatives in Matter in Extreme Conditions

Siegfried H. Glenzer (SLAC)

December 11, 2013

Presentation to: **2013 FUSION POWER ASSOCIATES**
34th Annual Meeting and Symposium

U.S. DEPARTMENT OF ENERGY
Office of Science

SLAC NATIONAL ACCELERATOR LABORATORY

Outline

- LCLS Free Electron Laser facility.
  - Unprecedented capabilities at the MEC instrument [since 4/2012]
    - 10^{12} x-ray photons for pump-prober experiments
    - High spectral resolution (seeded beam)
    - High wavenumber resolution (x-ray laser)
    - High temporal resolution (20-50 fs)
- Novel X-ray scattering experiments
  - First observation of Plasmon shift in shock-compressed plasmas
  - First continuous measurements of the dynamic structure factor
  - First observations of ion acoustic waves in warm dense plasmas
    - Pressures approaching 5-10 Mbar at 3x compressed Al
    - Test theoretical methods to determine pressures of dense matter
- Summary
    - High power laser workshop and outlook towards a bright future

We have a new precision tool to measure physical properties and to make transformative discoveries in High-Energy Density physics

Three big science questions

Develop and apply precision pump-probe experiments with the world-class LCLS beam to answer the most important questions in high energy density (HED) science

- **Relativistic laser plasma interactions**:
  Uncover the physical mechanisms for ultra short pulse laser matter interactions, plasma heating and particle acceleration
- **Laboratory astrophysics***:*
  Ultra-high power optical lasers offer the unique opportunity to produce and characterize collision-less shocks, particle acceleration, and anti-matter plasmas
- **Strong shocks and High Pressure phenomena:**
  The use of LCLS will probe high pressure states found at the center of the large Jovian plants, the earth's deepest interior and in inertial confinement fusion with unprecedented precision

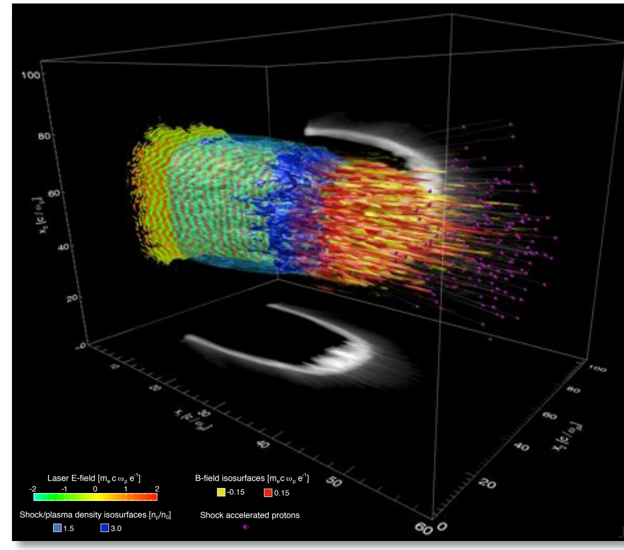

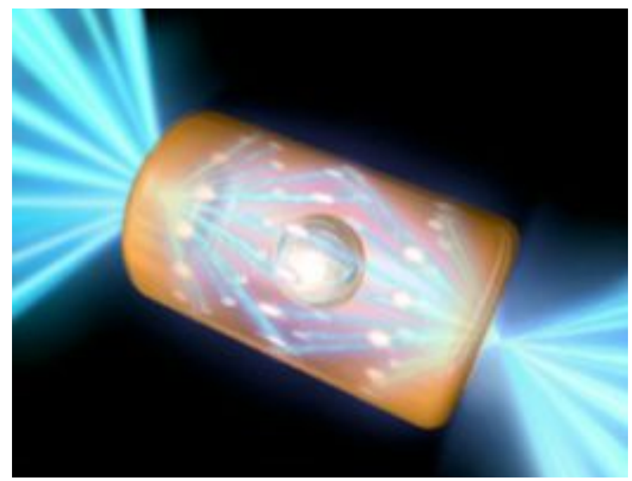

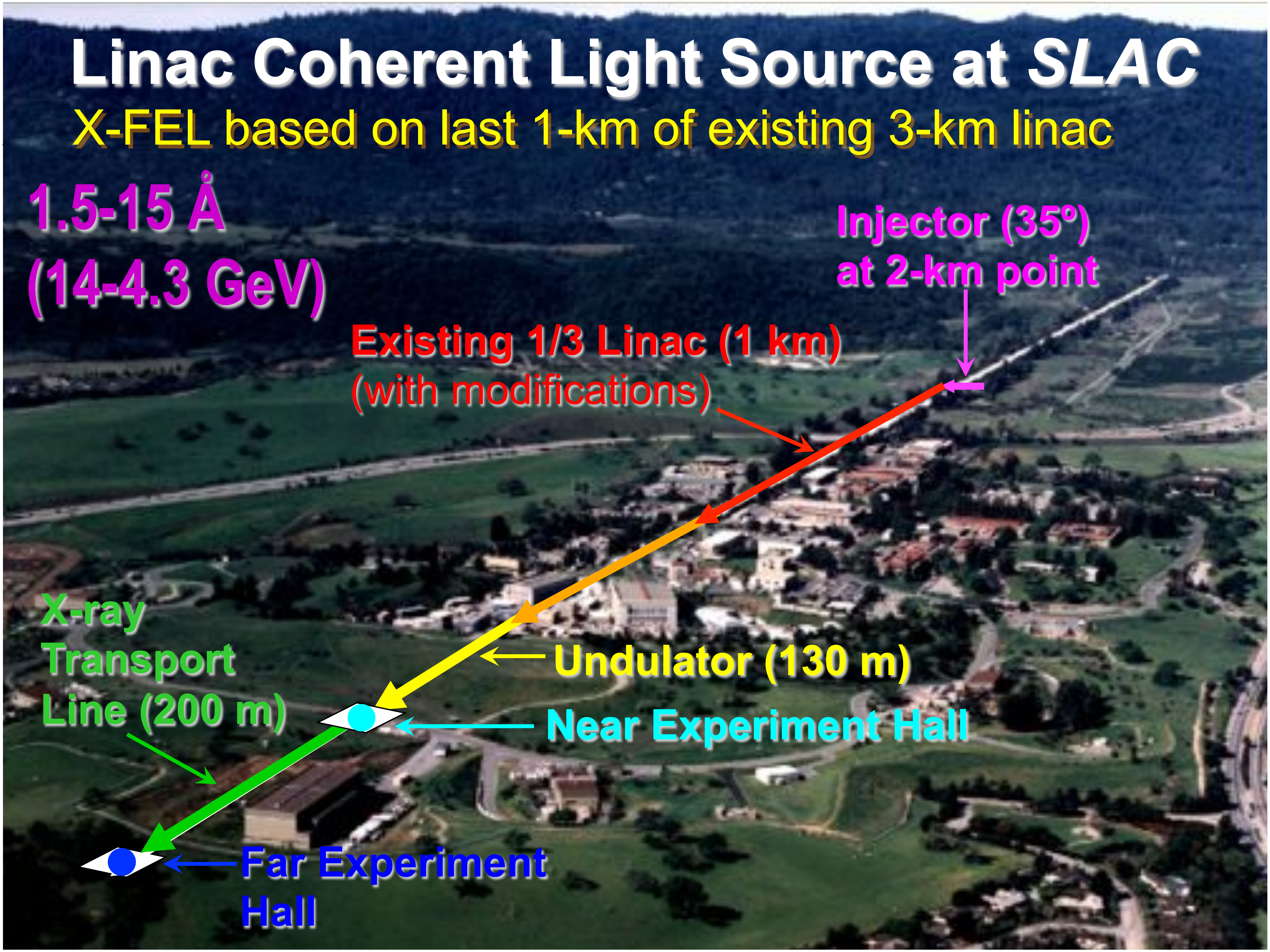
Linac Coherent Light Source at *SLAC*
X-FEL based on last 1-km of existing 3-km linac
1.5-15 Å
(14-4.3 GeV)
Injector (35º)
at 2-km point
Existing 1/3 Linac (1 km)
(with modifications)
Undulator (130 m)
X-ray
Transport
Line (200 m)
Near Experiment Hall
Far Experiment
Hall

Experiments at the Matter at Extreme Conditions end station

Matter of Extreme conditions end station

Tracking shock waves in dense matter

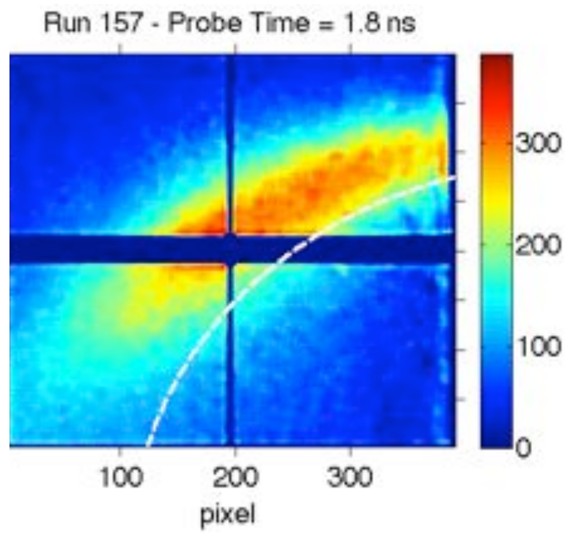

Shock wave driven by nanosecond laser

Precision X-ray Thomson scattering

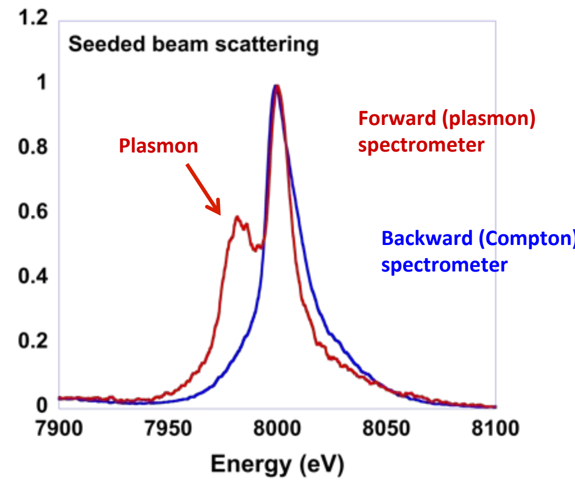

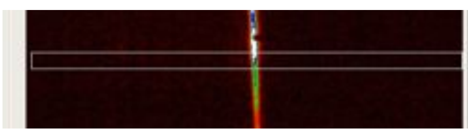

We perform novel pump-probe measurements of plasma conditions and shocks with 1 μm, 30 fs resolution

Experimental geometry uses counter propagating long pulse lasers and a delayed LCLS beam

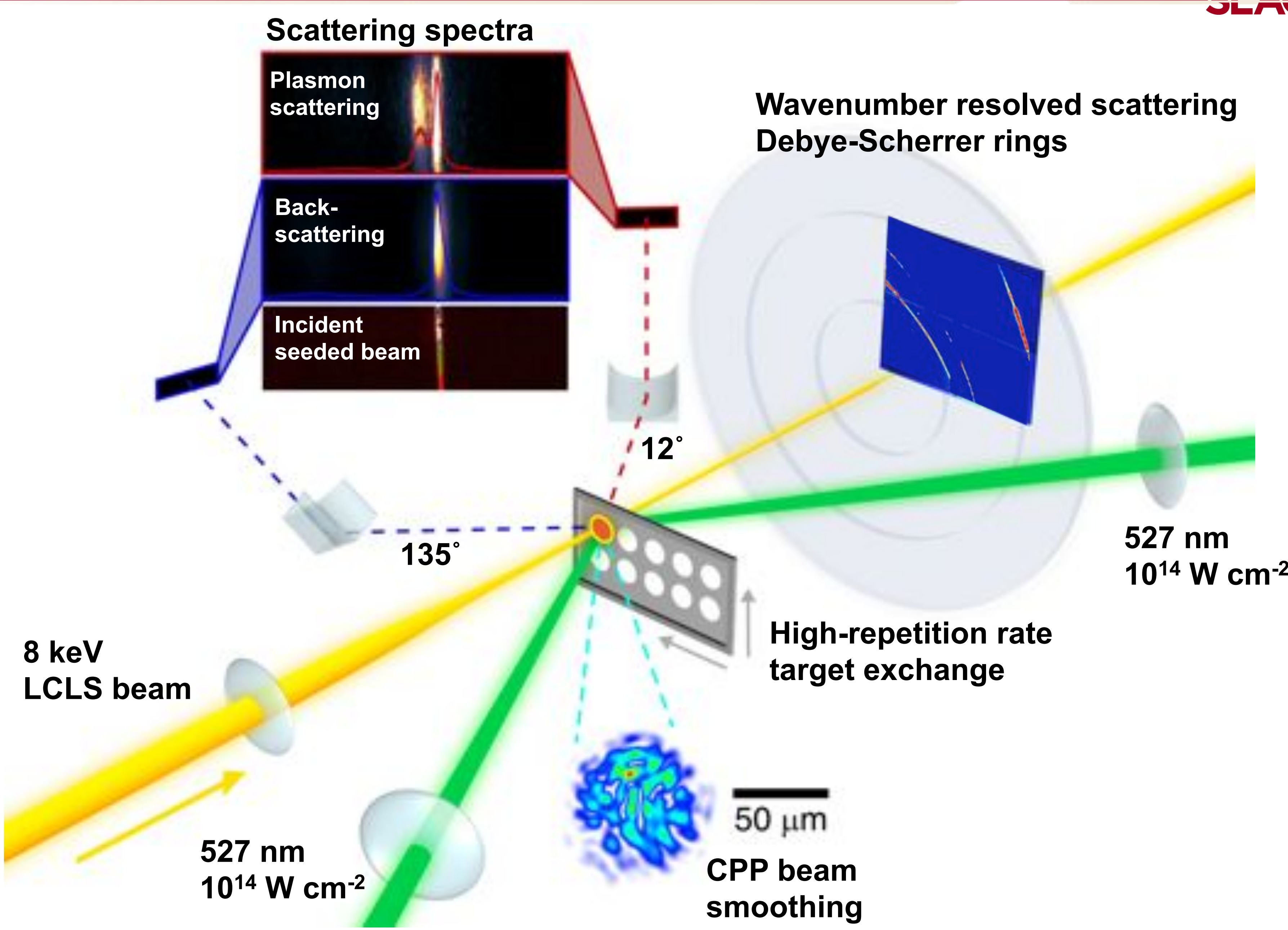

Experimental geometry uses counter propagating long pulse lasers and a delayed LCLS beam

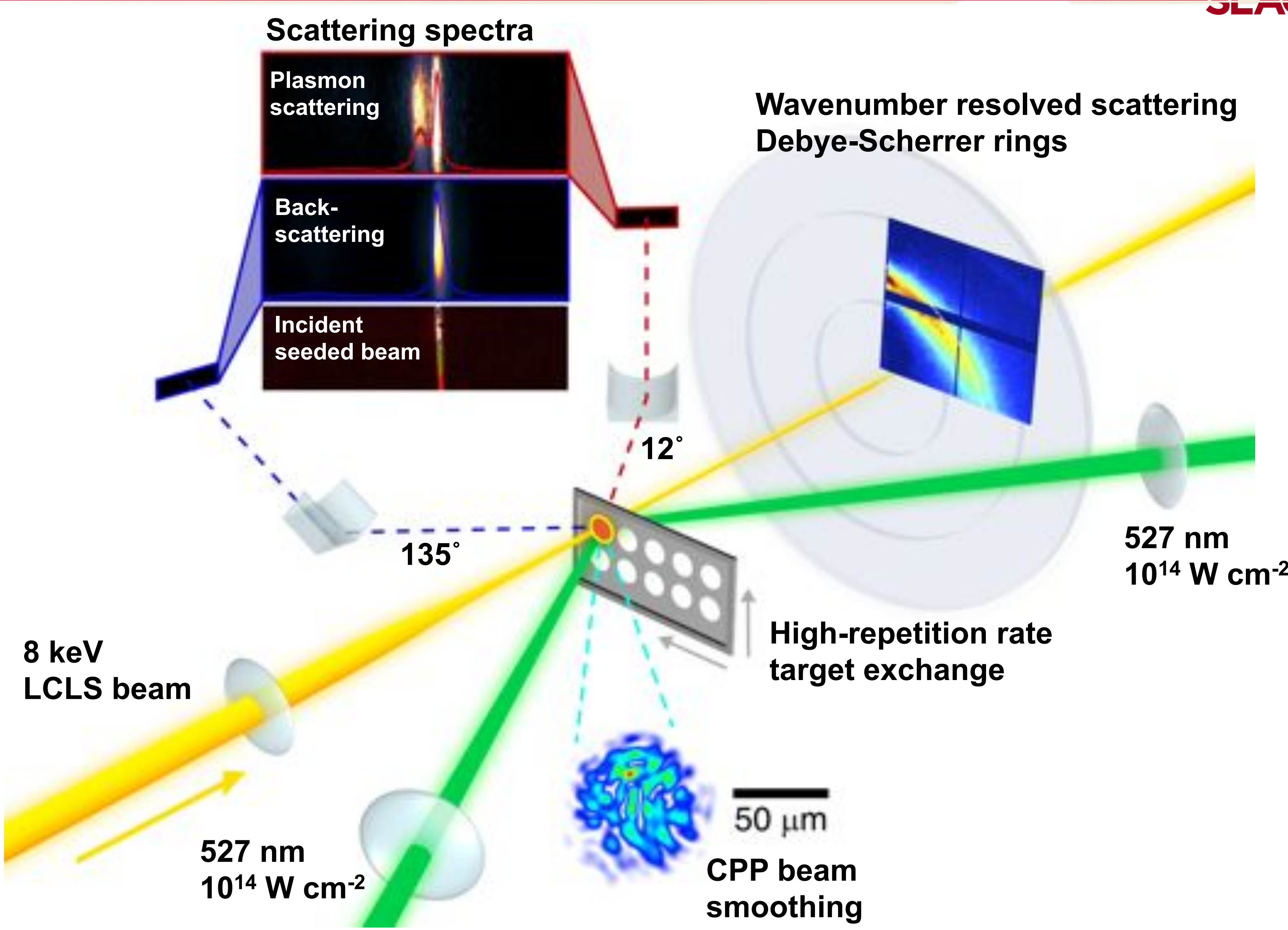

High resolution x-ray scattering observations of plasmons in Al using the seeded beam at 8 keV

SLAC

X-ray scattering from isochorically heated Al with seeded beam resolves plasmons

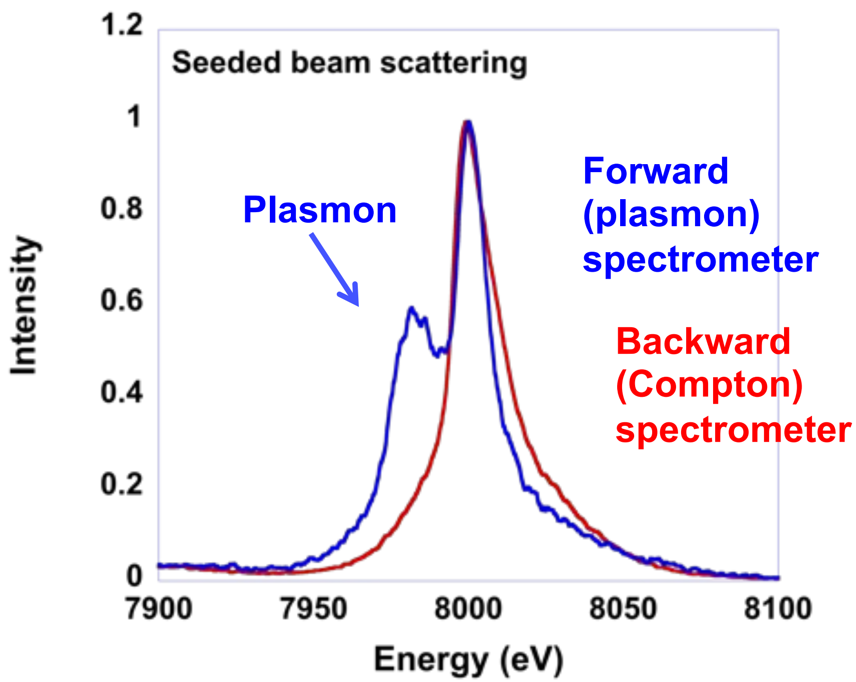

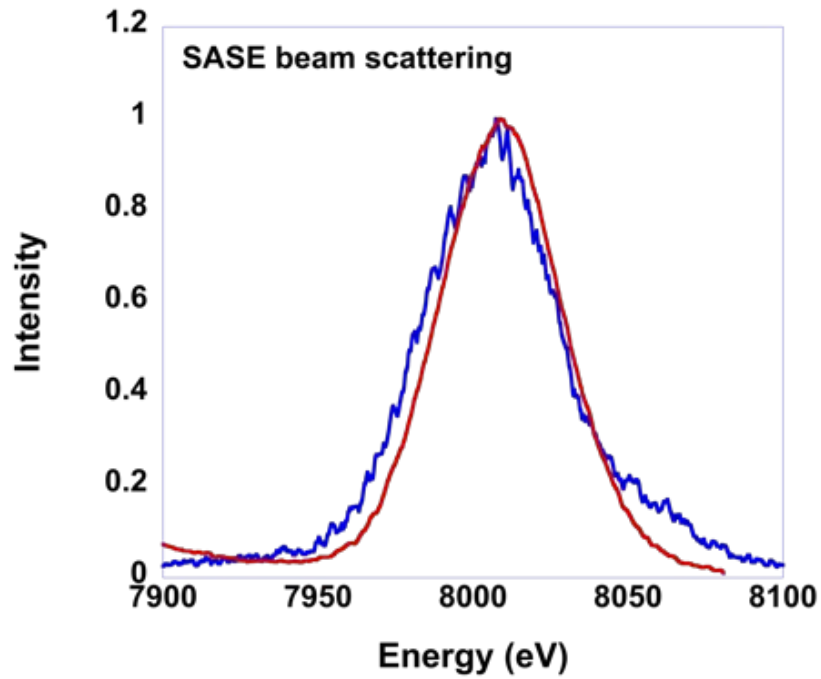

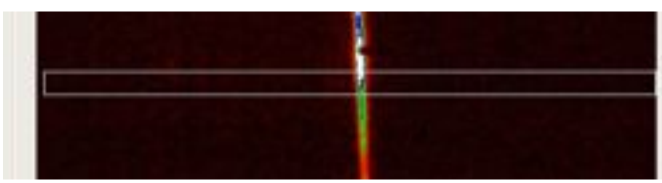

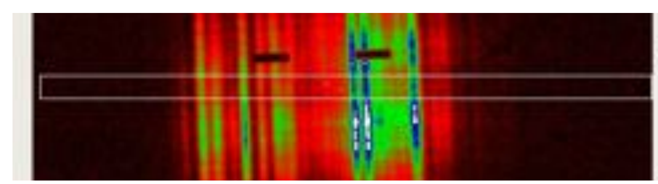

Seeded | **Bent crystal spectrometer in MEC** | **SASE**

High resolution x-ray scattering observations of plasmons in Al using the seeded beam at 8 keV

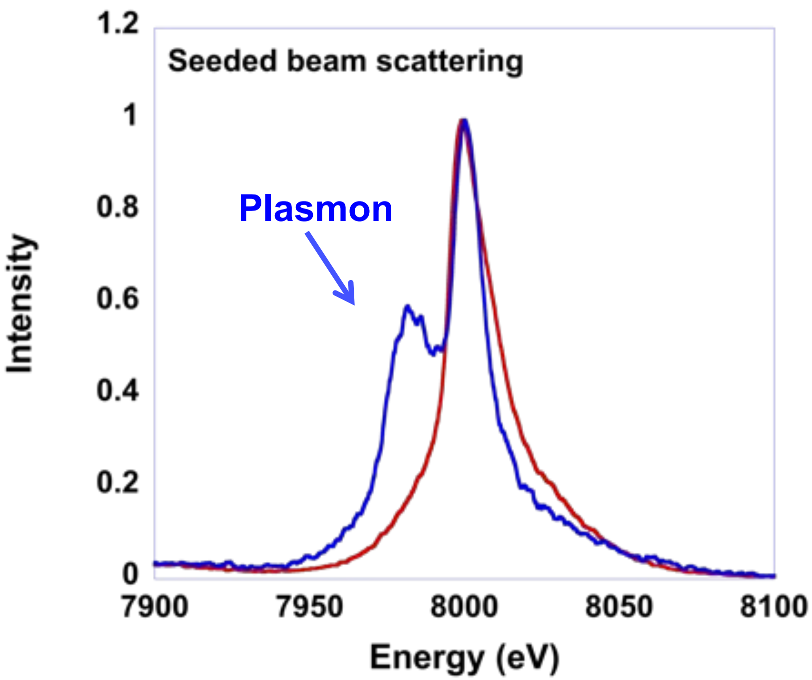

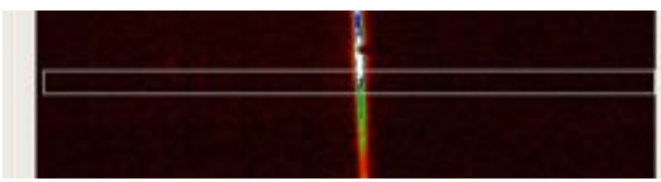

Seeded

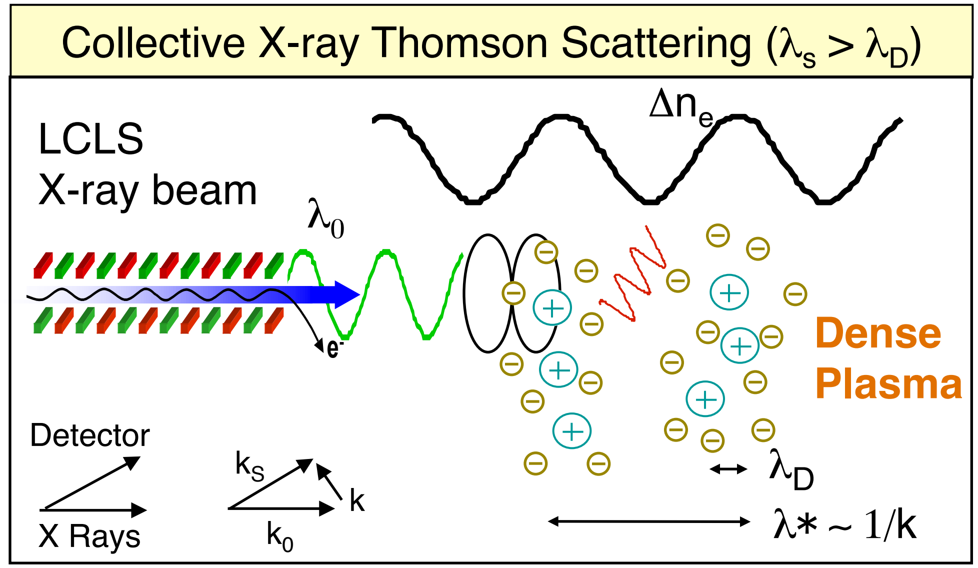

- Plasmon resonance determined by plasma frequency $\omega_{pe} = [n_e e^2/m_e \varepsilon_0]^{1/2}$
    - Glenzer et al., 2007 PRL
    - Kritcher et al., 2008 Science

- First observation of acoustic resonances at $\omega_{ac} \sim [kT_e/m_i]^{1/2}$

High resolution x-ray scattering observations of plasmons in Al using the seeded beam at 8 keV

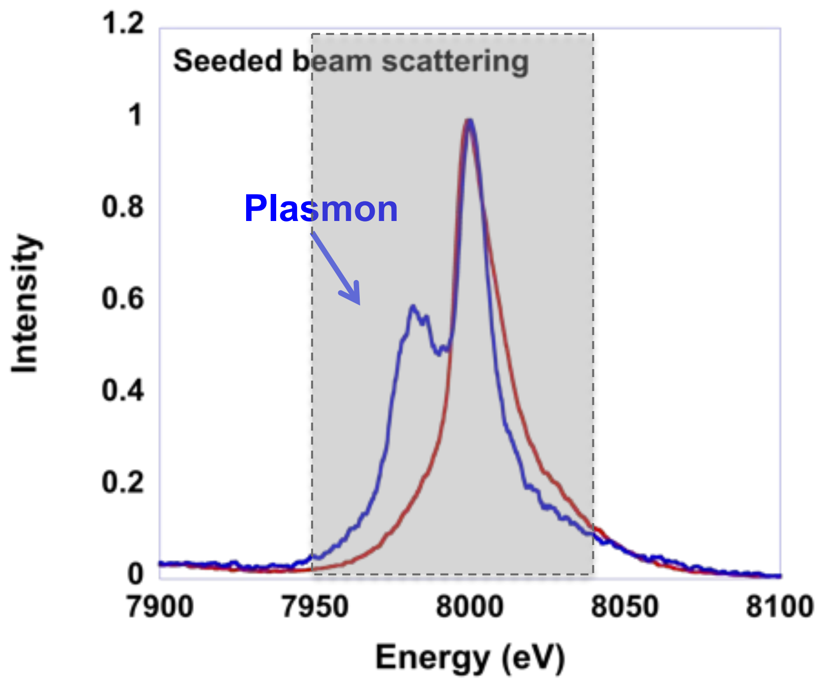

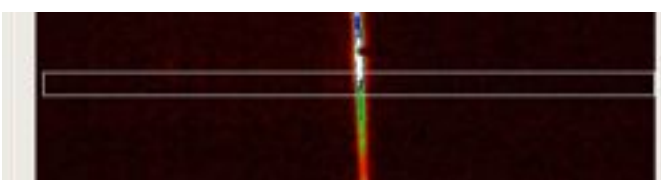

Seeded

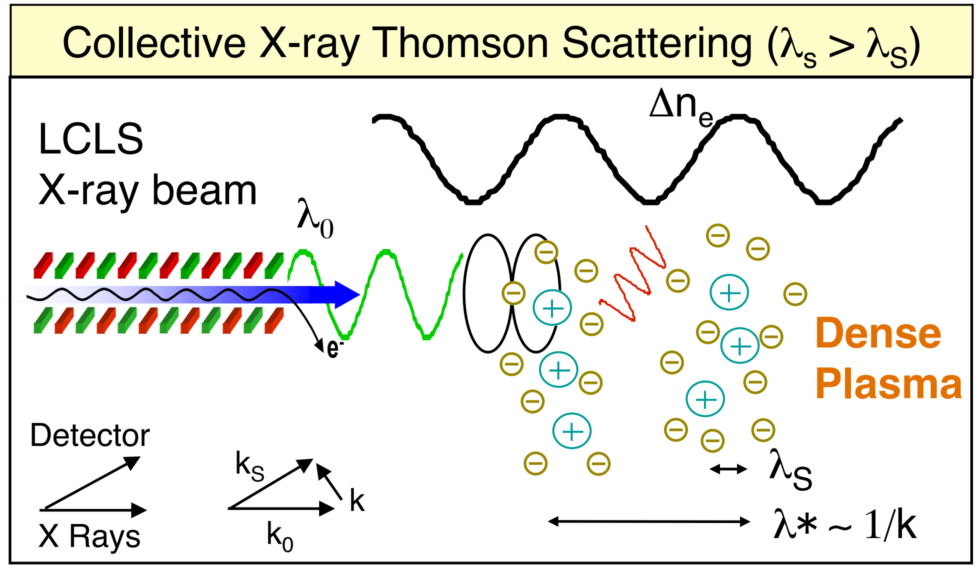

- Plasmon resonance determined by plasma frequency $\omega_{pe} = [n_e e^2/m_e \varepsilon_0]^{1/2}$
  - Glenzer et al., 2007 PRL
  - Kritcher et al., 2008 Science
- First observation of acoustic resonances at $\omega_{ac} \sim [kT_e/m_i]^{1/2}$

Theoretical fit to the plasmon spectrum determines solid- density conditions

SLAC

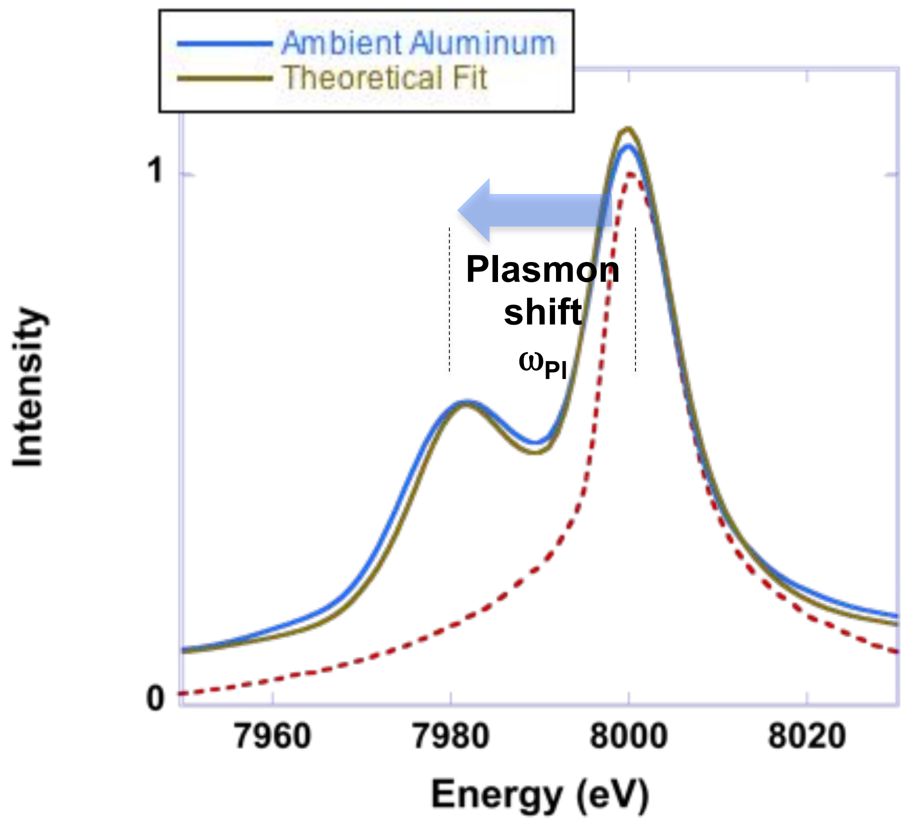

Total cross-section includes free, tightly, and weakly bound states

$$\frac{\partial^2\sigma}{\partial\Omega\partial\omega} = \sigma_T \frac{k_1}{k_o} S(k,\omega)$$

$$S(k,\omega) =$$

Ion Feature:

$$\left|f_1(k) + q(k)\right|^2 S_{ii}(k,\omega)$$

Electron Feature:

Bound-Free Feature:

Theoretical fit to the plasmon spectrum determines solid- density conditions

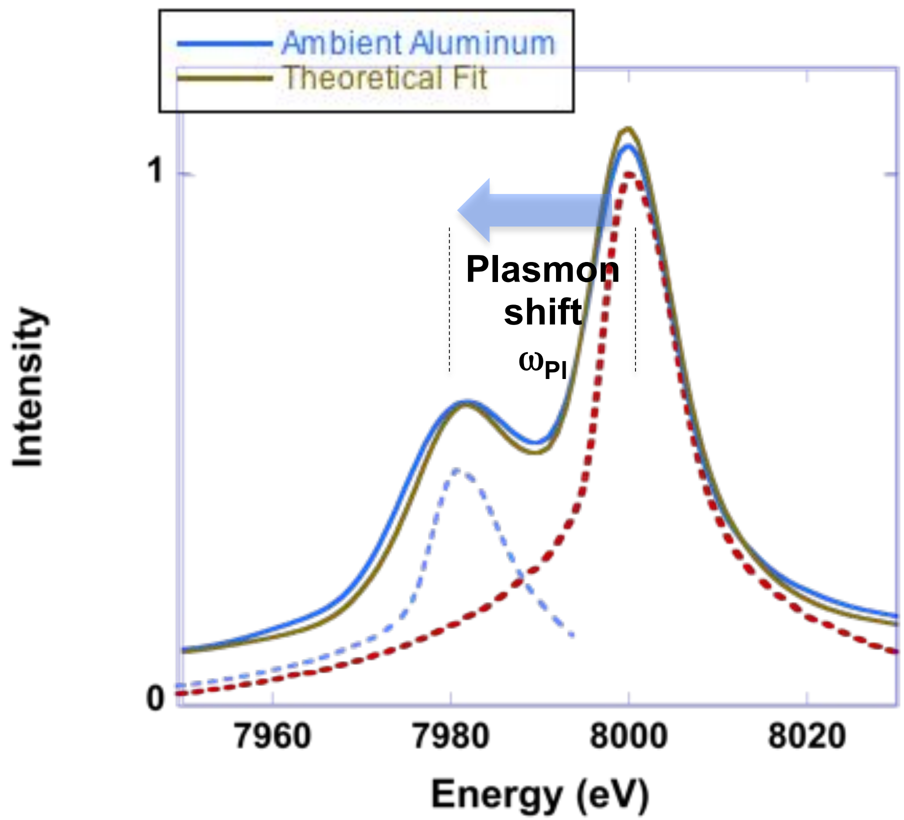

Total cross-section includes free, tightly, and weakly bound states

$$\frac{\partial^2\sigma}{\partial\Omega\partial\omega} = \sigma_T \frac{k_1}{k_o} S(k,\omega)$$

$$S(k,\omega) =$$

Ion Feature:

$$\left|f_1(k) + q(k)\right|^2 S_{ii}(k,\omega)$$

Electron Feature:

$$+Z_f S^o_{ee}(k,\omega)$$

Bound-Free Feature:

$$+Z_c \int \tilde{S}_{ce}(k,\omega-\omega')S_{ce}(k,\omega')\partial\omega'$$

We now have an accurate (first-principals) method that determines the physical properties of warm dense matter: n_e= 1.8 x 10^{23} cm^{-3} ± 5%

Theoretical fit to the plasmon spectrum determines solid- density conditions

SLAC

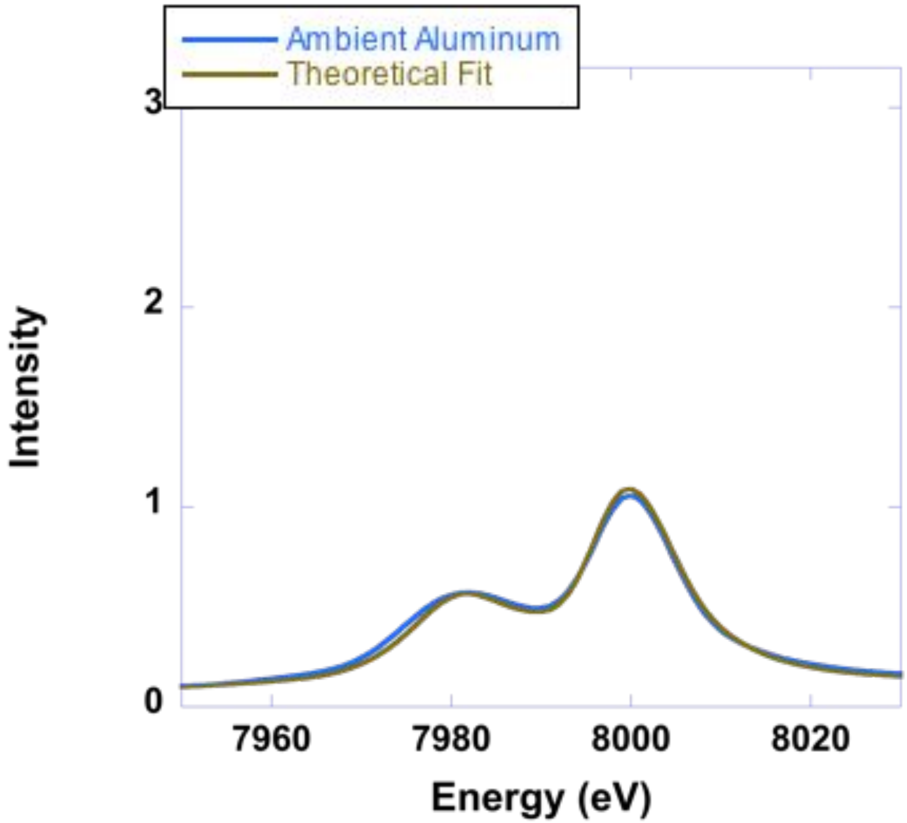

Total cross-section includes free, tightly, and weakly bound states

$$\frac{\partial^2\sigma}{\partial\Omega\partial\omega} = \sigma_T \frac{k_1}{k_o} S(k,\omega)$$

$$S(k,\omega) =$$

Ion Feature:

$$\left| f_1(k) + q(k) \right|^2 S_{ii}(k,\omega)$$

Electron Feature:

$$+Z_f S_{ee}^o(k,\omega)$$

Bound-Free Feature:

$$+Z_c \int \tilde{S}_{ce}(k,\omega-\omega') S_{ce}(k,\omega') \partial\omega'$$

Plasmon measurements accurately determine 3x compressed Al at temperatures of 2.5 eV

SLAC

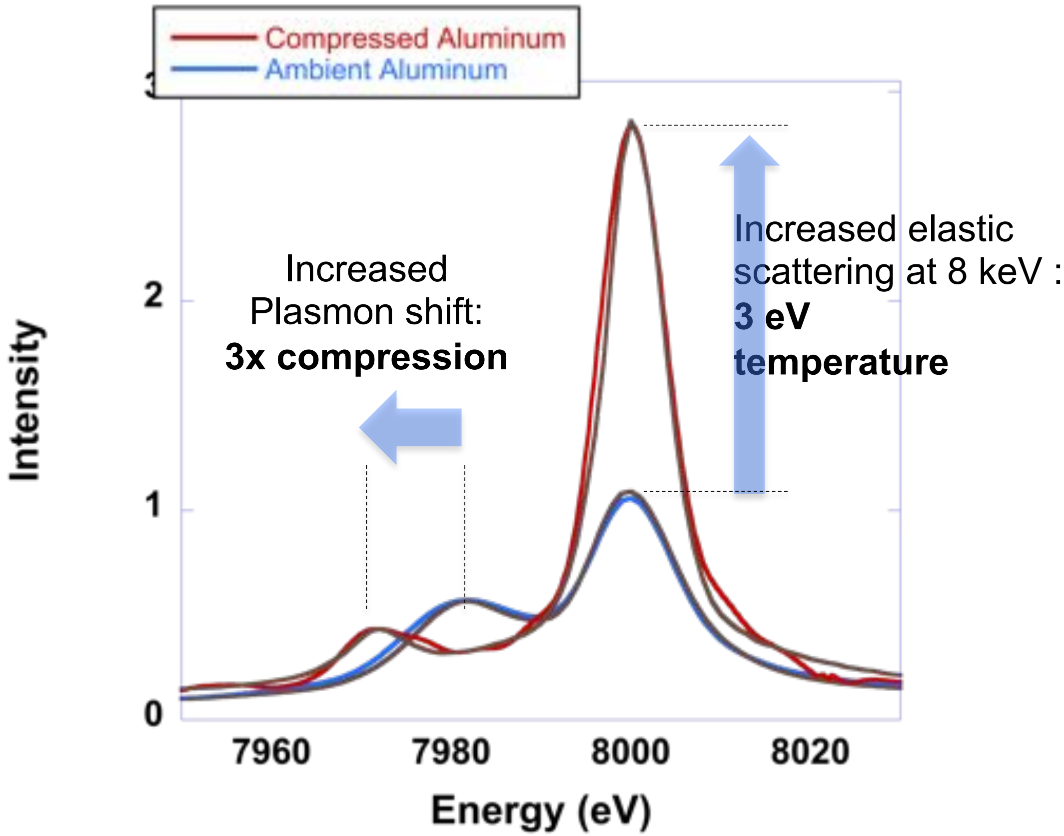

Total cross-section includes free, tightly, and weakly bound states

$$\frac{\partial^2\sigma}{\partial\Omega\partial\omega} = \sigma_T \frac{k_1}{k_o} S(k,\omega)$$

$$S(k,\omega) =$$

Ion Feature:

$$\left|f_1(k) + q(k)\right|^2 S_{ii}(k,\omega)$$

Electron Feature:

$$+Z_f S_{ee}^o(k,\omega)$$

Bound-Free Feature:

$$+Z_c \int \tilde{S}_{ce}(k,\omega-\omega') S_{ce}(k,\omega')\partial\omega'$$

We now have an accurate (first-principals) method that determines the physical properties of warm dense matter: n_e= 4.7 x 10^{23} cm^{-3} ± 5%

First Observation of ion-acoustic waves in Warm Dense Matter

Al @ $\rho=7.0\pm0.9$ g/cm^3
$\Omega=152 \pm 13$ meV

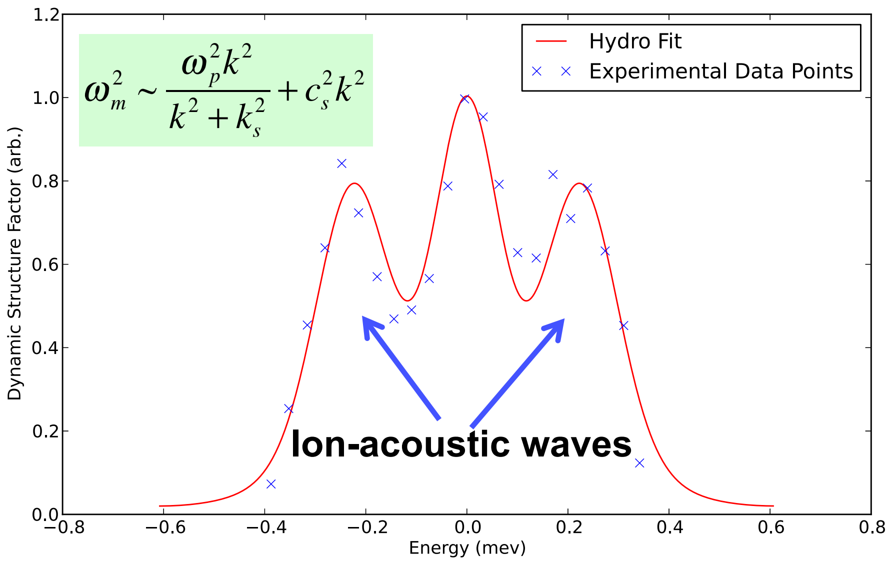

$2\theta=30^o$, $Q=2.1$ Å^{-1}
$Q_0=3.7\pm0.1$ Å^{-1}; $Q/Q_0=0.57$

G. Monaco, J. Hastings, G. Gregori et al., unpublished

Monochromator for LCLS beam:
Si(4,4,4): $\Delta E/E = 5 \times 10^{-6}$

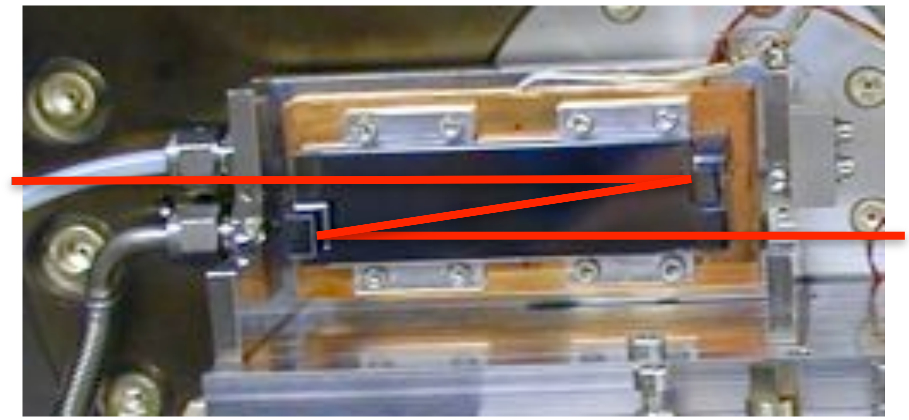

High-resolution crystal analyzer

diced Si(444) crystal
with R=1 m & $\theta=87°$
$\Rightarrow$
100 meV @ 7919 eV

Clear evidence of double shock compression at the time of shock coalescence by directly monitoring the ion-ion correlation peak

Bragg equation: $n\lambda = 2d \sin\theta$

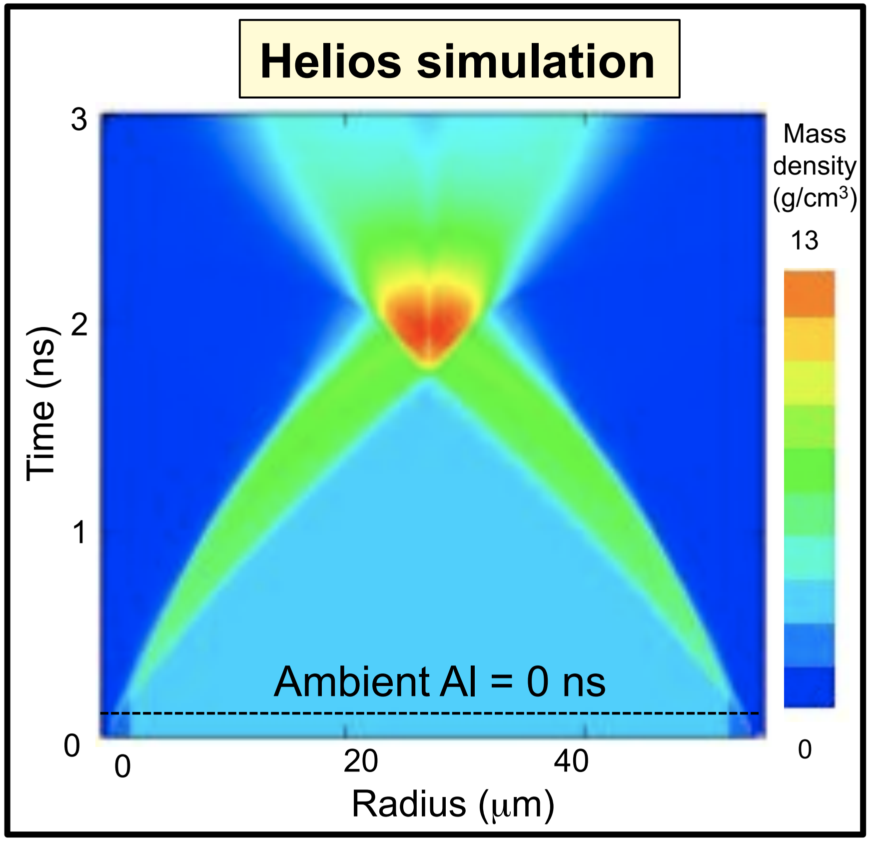

Radial lineout

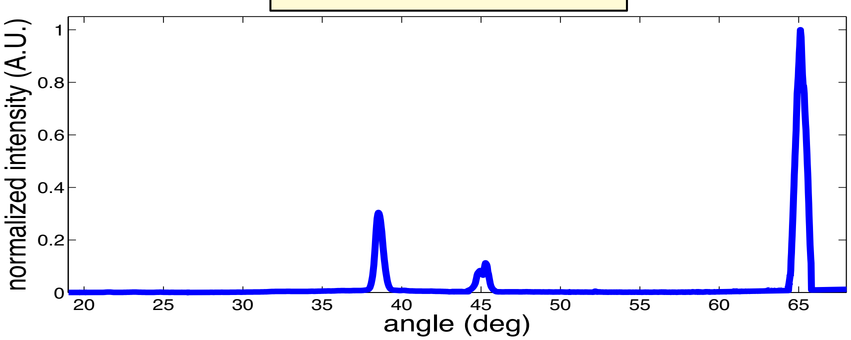

CSPAD detector

Shock coalescence = 1.9 ns

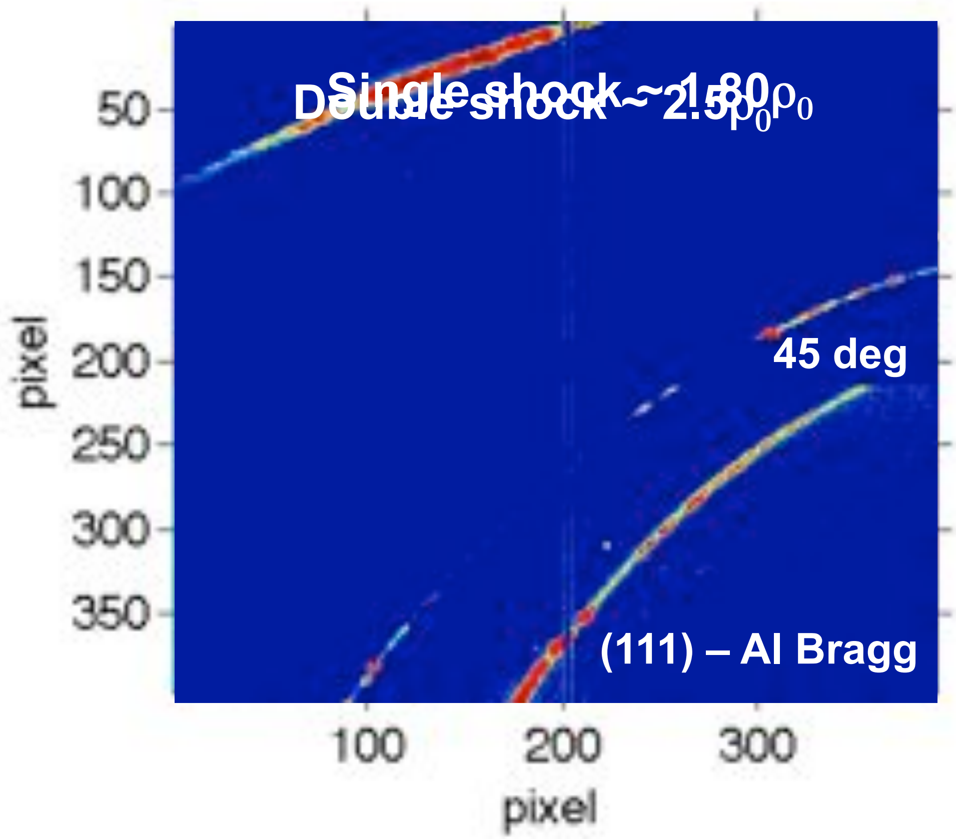

Bragg peaks in cold Al

Clear evidence of double shock compression at the time of shock coalescence by directly monitoring the ion-ion correlation peak

SLAC

Bragg equation: $n\lambda = 2d \sin\theta$

Helios simulation

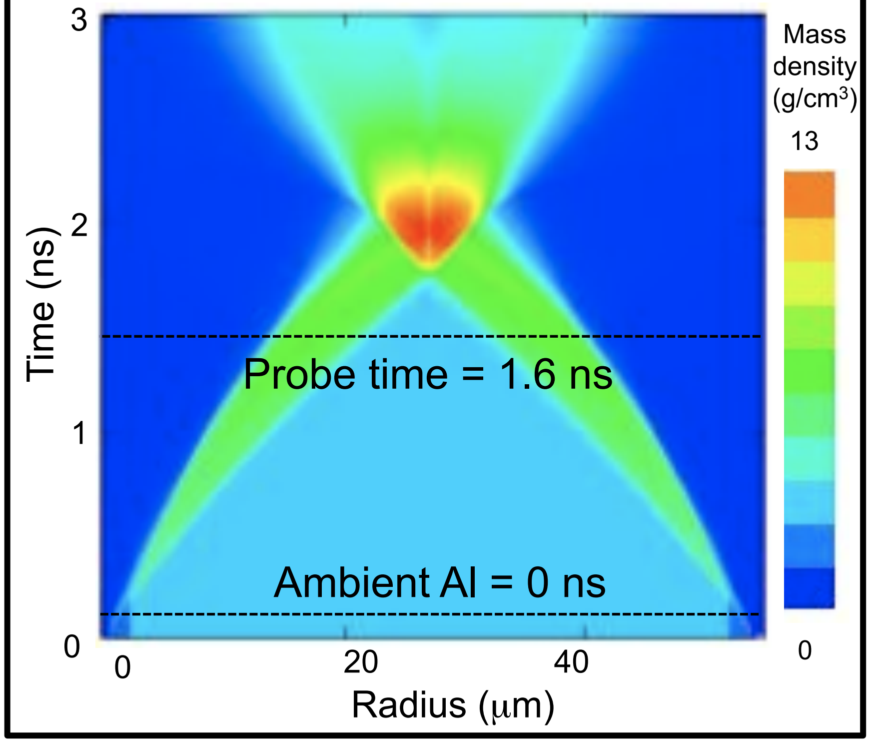

Radial lineout

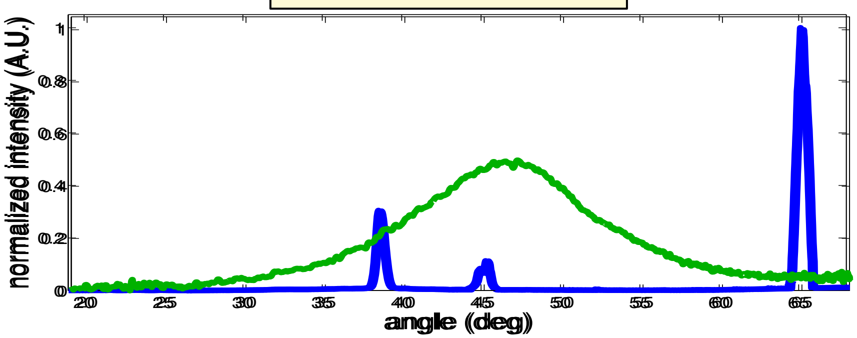

CSPAD detector

Probe time = 1.6 ns

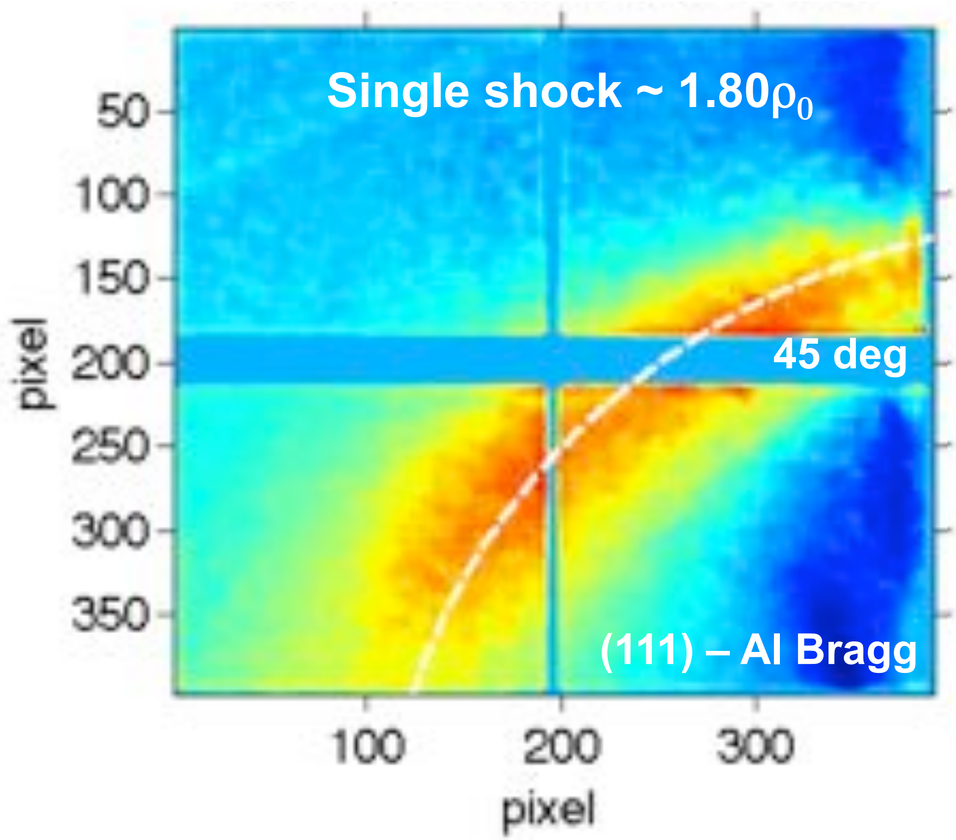

Ion-ion correlation peak

Clear evidence of double shock compression at the time of shock coalescence by directly monitoring the ion-ion correlation peak

Bragg equation: $n\lambda = 2d \sin\theta$

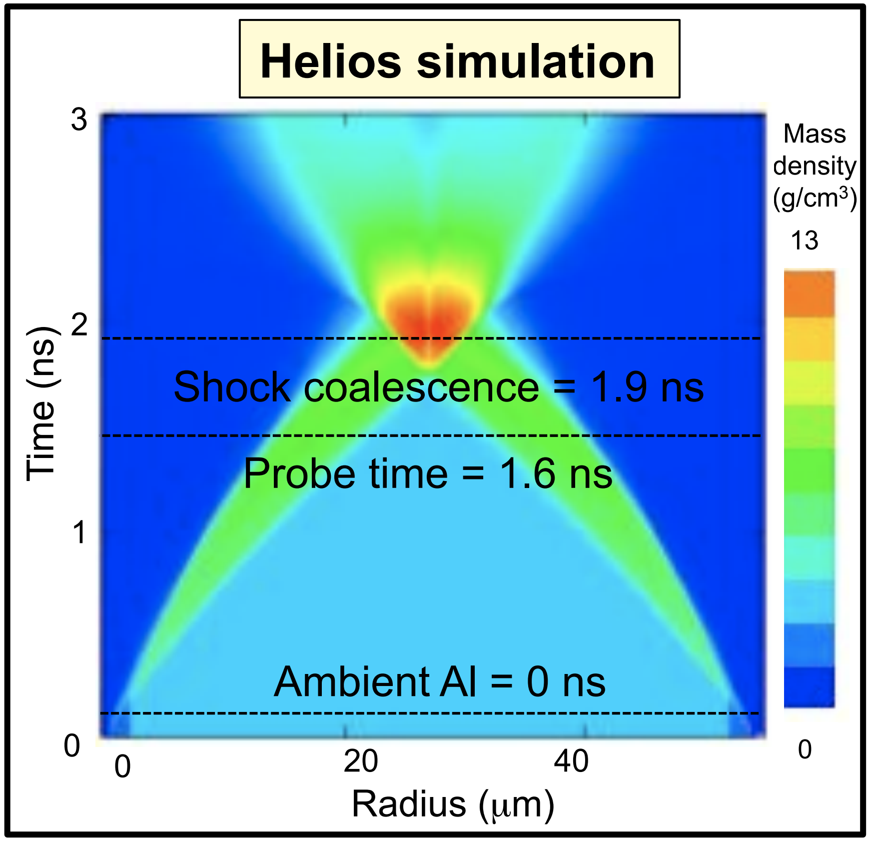

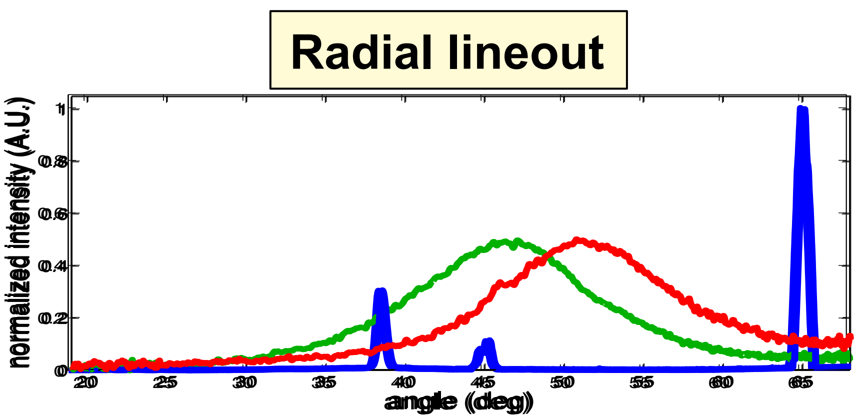

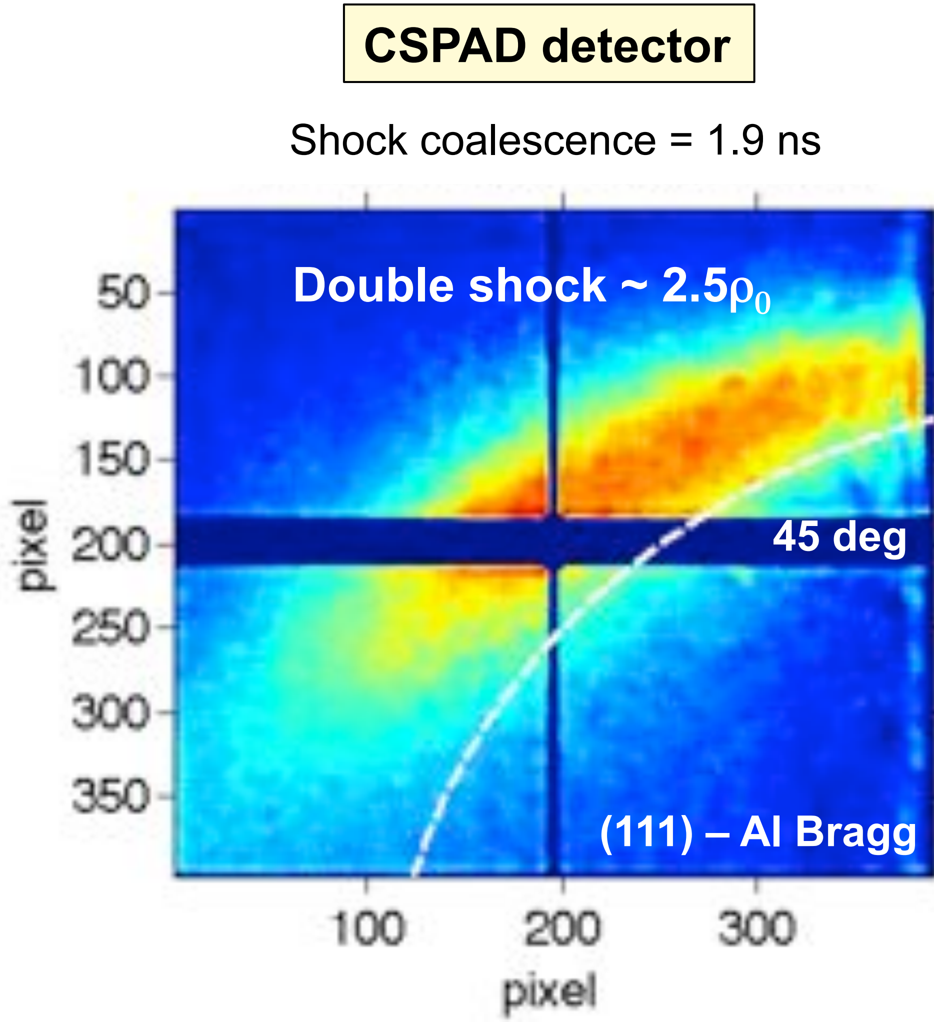

Shock coalescence

Wavenumber resolved scattering data resolves interactions on atomic scales

SLAC

Using short range repulsion provides an excellent fit to W(k)

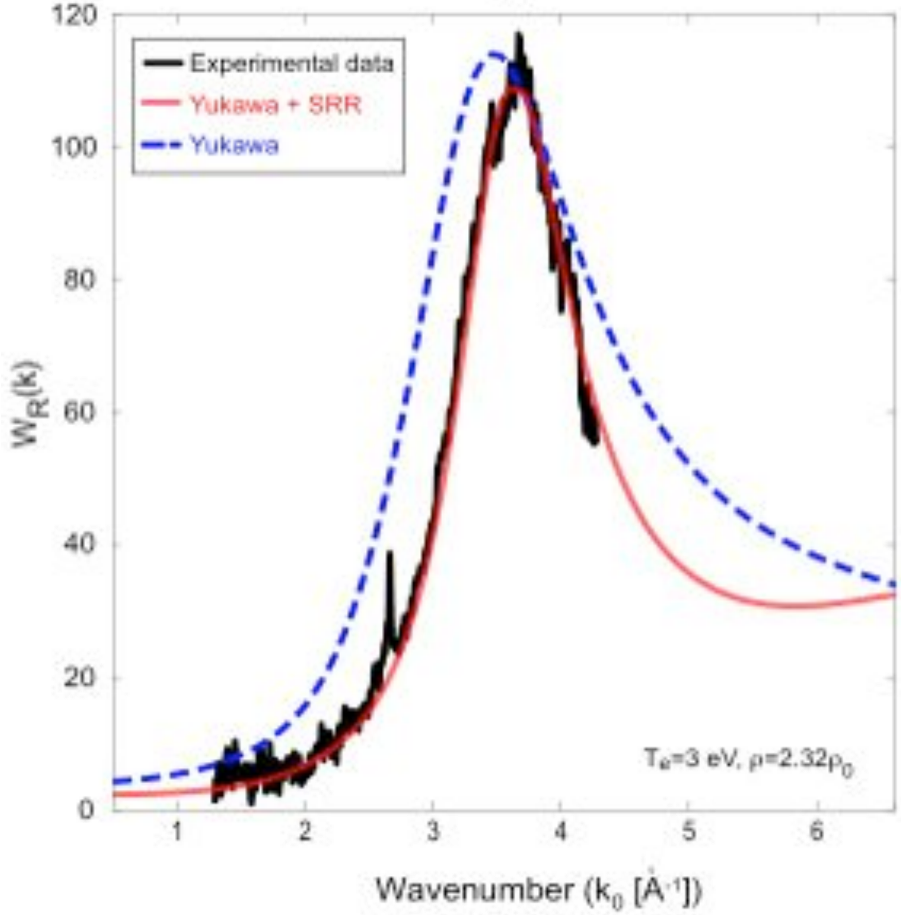

Pseudopotentials account for polarisable free electron background & bound core electrons

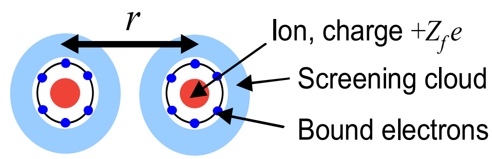

$$\beta V_{ii}(r) = \frac{Z_f^2 e^2}{r k_B T} e^{-\kappa_e r} + \frac{\sigma^4}{r^4}$$

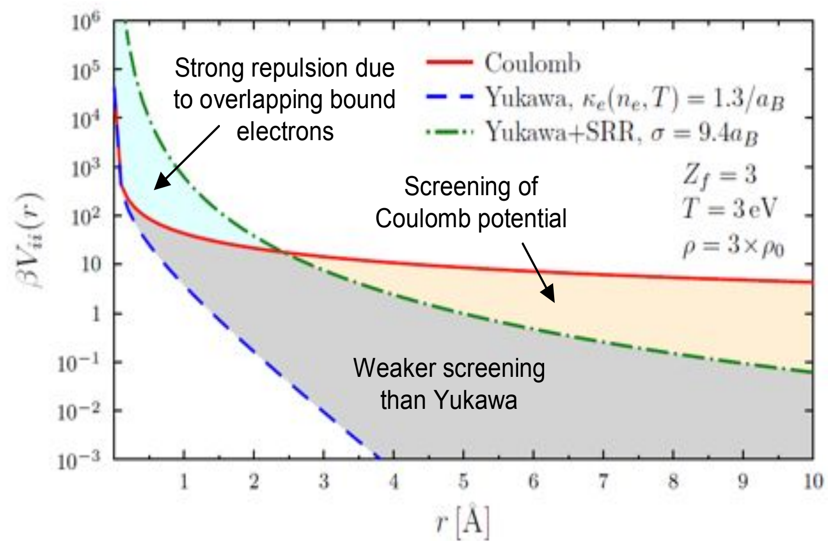

Combined with plasmon data these experiments yield a critical experimental test

Angularly and spectrally resolved data show that the shift of $W_R(k)$ is determined by short range repulsion

SLAC

Ion-ion correlation peak position vs compression

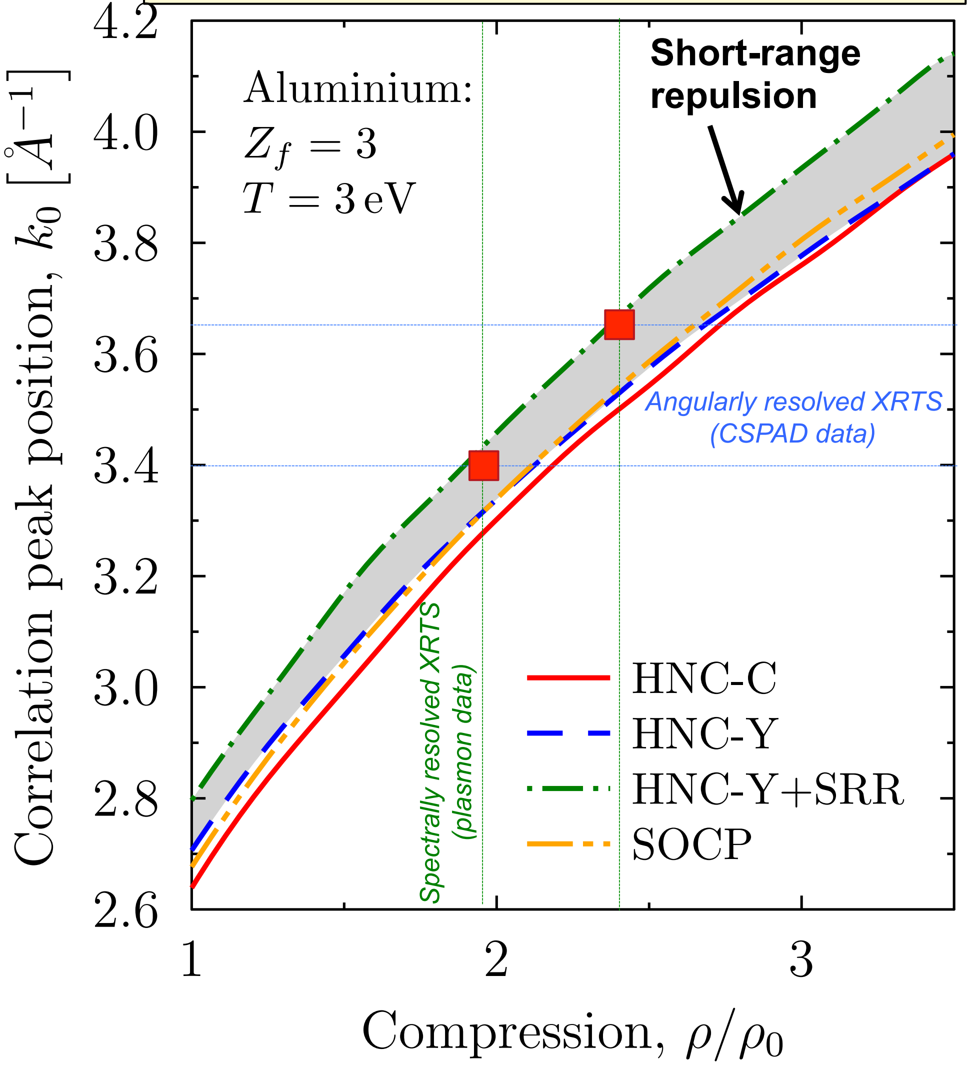

- **The peak of the ion-ion structure factor provides a well pronounced diagnostic feature**
- **After calibration against plasmon scattering the wavenumber of the maximum of W(k) can be used to infer densities**
- **Short range repulsion is an indication of negative screening**
- **Important consequences when determining the pressure**

The internal energy per particle (and consequently the pressure) depends on S(k)

SLAC

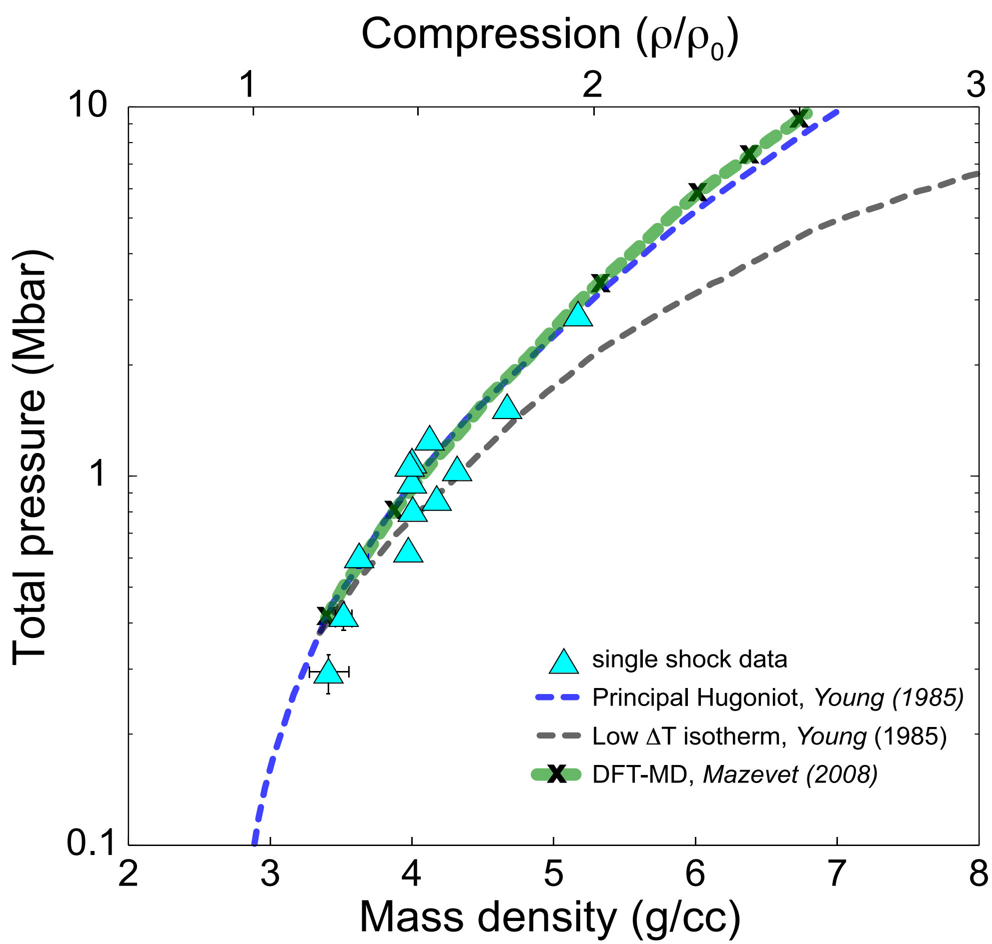

Total pressure - P(n_e,T_e,S(k))

$$P_{TOT} = P_i + P_e$$

Ion pressure

$$P_i = p^x + P_G$$

Excess ion pressure [1]

$$p^x = \frac{n_i U^{(0)}}{3N} - \frac{n_i (Ze)^2}{12\pi^2}\int_0^\infty S(k)\frac{k_e^4}{(k^2+k_e^2)^2}\partial k$$

Ideal gas pressure

$$P_G = n_i k_B T_i$$

Electron pressure

$$P_e = P_F + P_{\deg} + P_C + P_{xc}$$

Fermi pressure [2]

$$P_F = \frac{h^2}{20m_e}\left(\frac{3}{\pi}\right)^{2/3} n_e^{5/3}$$

Quantum electron degeneracy pressure [1]

$$P_{\deg} = \frac{\pi m_e^4 c^5}{3h^3}\left[R(2R^2-3)\sqrt{1+R^2}+3\sinh^{-1}R\right] \quad R = \frac{P_F}{m_e c}$$

Coulomb negative pressure [1]

$$P_C = -\frac{8\pi^3 m_e^4 c^5}{h^3}\left[\frac{\alpha Z^{2/3}}{10\pi^2}\left(\frac{4}{9\pi}\right)^{1/3}\right]R^4 \quad \alpha = \frac{e^2}{4\pi\varepsilon_0 \hbar c}$$

Electron-exchange pressure [1]

$$P_{xc} = -\frac{2\alpha m_e^4 c^5}{h^3}\beta^*$$

[1] Galam and Hansen, Phys Rev. A, 14 (1976)

[2] R. P. Drake, *High-Energy-Density Physics,* (2006)

The internal energy per particle (and consequently the pressure) depends on S(k)

SLAC

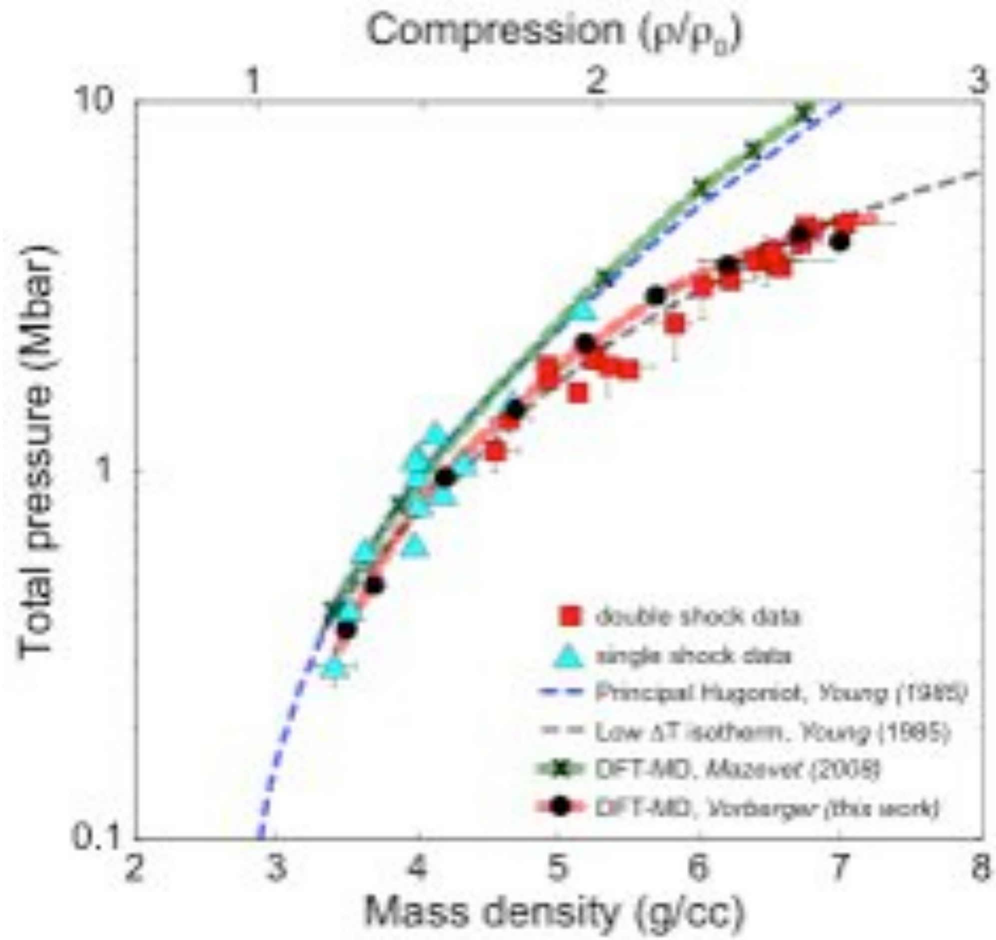

Total pressure - P(n$_e$,T$_e$,S(k))

$$P_{TOT} = P_i + P_e$$

Ion pressure

$$P_i = p^x + P_G$$

Excess ion pressure [1]

$$p^x = \frac{n_i U^{(0)}}{3N} - \frac{n_i (Ze)^2}{12\pi^2} \int_0^\infty S(k) \frac{k_e^4}{(k^2 + k_e^2)^2} \partial k$$

Ideal gas pressure

$$P_G = n_i k_B T_i$$

Electron pressure

$$P_e = P_F + P_{\deg} + P_C + P_{xc}$$

Fermi pressure [2]

$$P_F = \frac{h^2}{20 m_e} \left(\frac{3}{\pi}\right)^{2/3} n_e^{5/3}$$

Quantum electron degeneracy pressure [1]

$$P_{\deg} = \frac{\pi m_e^4 c^5}{3h^3} \left[R(2R^2 - 3)\sqrt{1 + R^2} + 3\sinh^{-1} R \right] \quad R = \frac{P_F}{m_e c}$$

Coulomb negative pressure [1]

$$P_C = -\frac{8\pi^3 m_e^4 c^5}{h^3} \left[\frac{\alpha Z^{2/3}}{10\pi^2} \left(\frac{4}{9\pi}\right)^{1/3} \right] R^4 \quad \alpha = \frac{e^2}{4\pi\varepsilon_0 \hbar c}$$

Electron-exchange pressure [1]

$$P_{xc} = -\frac{2\alpha m_e^4 c^5}{h^3} \beta^*$$

[1] Galam and Hansen, Phys Rev. A, 14 (1976)

[2] R. P. Drake, *High-Energy-Density Physics,* (2006)

The internal energy per particle (and consequently the pressure) depends on S(k)

Can account for as much as -2 Mbar

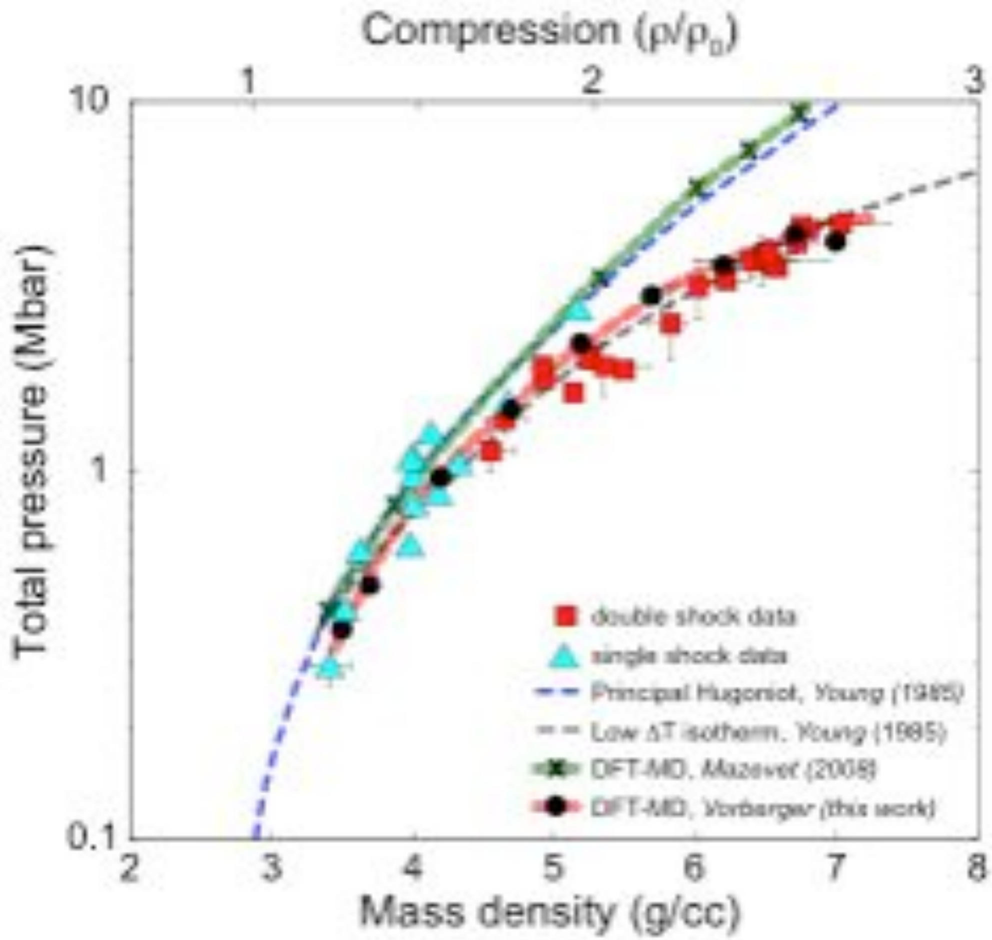

Total pressure - $P(n_e, T_e, S(k))$

$$P_{TOT} = P_i + P_e$$

Ion pressure

$$P_i = p^x + P_G$$

Excess ion pressure [1]

$$p^x = \frac{n_i U^{(0)}}{3N} - \frac{n_i (Ze)^2}{12\pi^2} \int_0^\infty S(k) \frac{k_e^4}{(k^2 + k_e^2)^2} \partial k$$

Ideal gas pressure

$$P_G = n_i k_B T_i$$

Electron pressure

$$P_e = P_F + P_{\deg} + P_C + P_{xc}$$

Fermi pressure [2]

$$P_F = \frac{h^2}{20 m_e} \left(\frac{3}{\pi} \right)^{2/3} n_e^{5/3}$$

Quantum electron degeneracy pressure [1]

$$P_{\deg} = \frac{\pi m_e^4 c^5}{3h^3} \left[R(2R^2 - 3)\sqrt{1 + R^2} + 3\sinh^{-1} R \right] \quad R = \frac{P_F}{m_e c}$$

Coulomb negative pressure [1]

$$P_C = -\frac{8\pi^3 m_e^4 c^5}{h^3} \left[\frac{\alpha Z^{2/3}}{10\pi^2} \left(\frac{4}{9\pi} \right)^{1/3} \right] R^4 \quad \alpha = \frac{e^2}{4\pi\varepsilon_0 \hbar c}$$

Electron-exchange pressure [1]

$$P_{xc} = -\frac{2\alpha m_e^4 c^5}{h^3} \beta^*$$

[1] Galam and Hansen, Phys Rev. A, 14 (1976)

[2] R. P. Drake, *High-Energy-Density Physics,* (2006)

The internal energy per particle (and consequently the pressure) depends on S(k)

Can account for as much as -2 Mbar

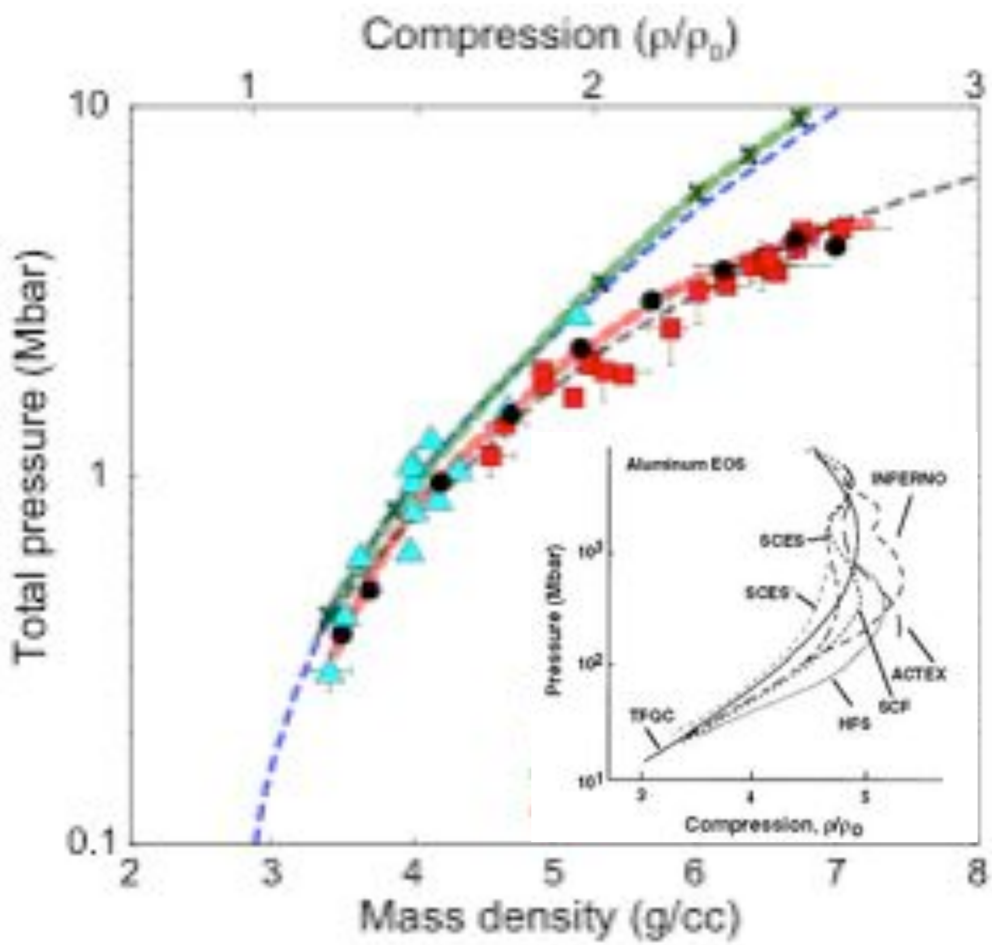

Total pressure - $P(n_e, T_e, S(k))$

$$P_{TOT} = P_i + P_e$$

Ion pressure

$$P_i = p^x + P_G$$

Excess ion pressure [1]

$$p^x = \frac{n_i U^{(0)}}{3N} - \frac{n_i (Ze)^2}{12\pi^2} \int_0^\infty S(k) \frac{k_e^4}{(k^2 + k_e^2)^2} \partial k$$

Ideal gas pressure

$$P_G = n_i k_B T_i$$

Electron pressure

$$P_e = P_F + P_{\deg} + P_C + P_{xc}$$

Fermi pressure [2]

$$P_F = \frac{h^2}{20 m_e} \left(\frac{3}{\pi} \right)^{2/3} n_e^{5/3}$$

Quantum electron degeneracy pressure [1]

$$P_{\deg} = \frac{\pi m_e^4 c^5}{3h^3} \left[R(2R^2 - 3)\sqrt{1 + R^2} + 3\sinh^{-1} R \right] \quad R = \frac{P_F}{m_e c}$$

Coulomb negative pressure [1]

$$P_C = -\frac{8\pi^3 m_e^4 c^5}{h^3} \left[\frac{\alpha Z^{2/3}}{10\pi^2} \left(\frac{4}{9\pi} \right)^{1/3} \right] R^4 \quad \alpha = \frac{e^2}{4\pi\varepsilon_0 \hbar c}$$

Electron-exchange pressure [1]

$$P_{xc} = -\frac{2\alpha m_e^4 c^5}{h^3} \beta^*$$

[1] Galam and Hansen, Phys Rev. A, 14 (1976)

[2] R. P. Drake, *High-Energy-Density Physics,* (2006)

2 years versus 7 minutes

Measured ion-ion correlation peak

T. Ma *et al.*, *PRL 110, 065001 (2013)*

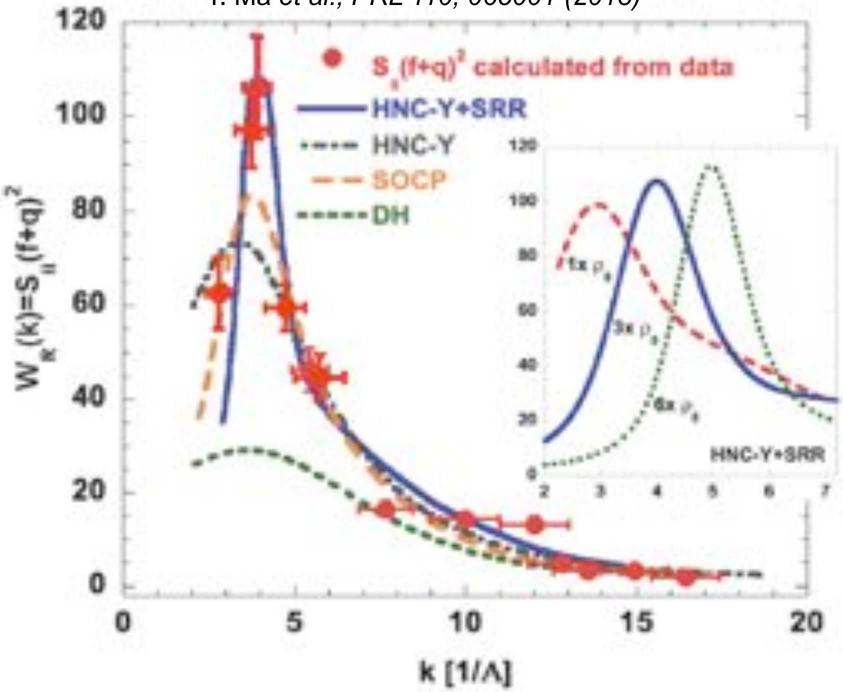

The shift and change in peak intensity of the correlation peak for 1.8x and 2.75x compressed aluminum, modeled using HNC-Y+SRR, can serve as a dynamic density diagnostic

Radial lineout (single shot)

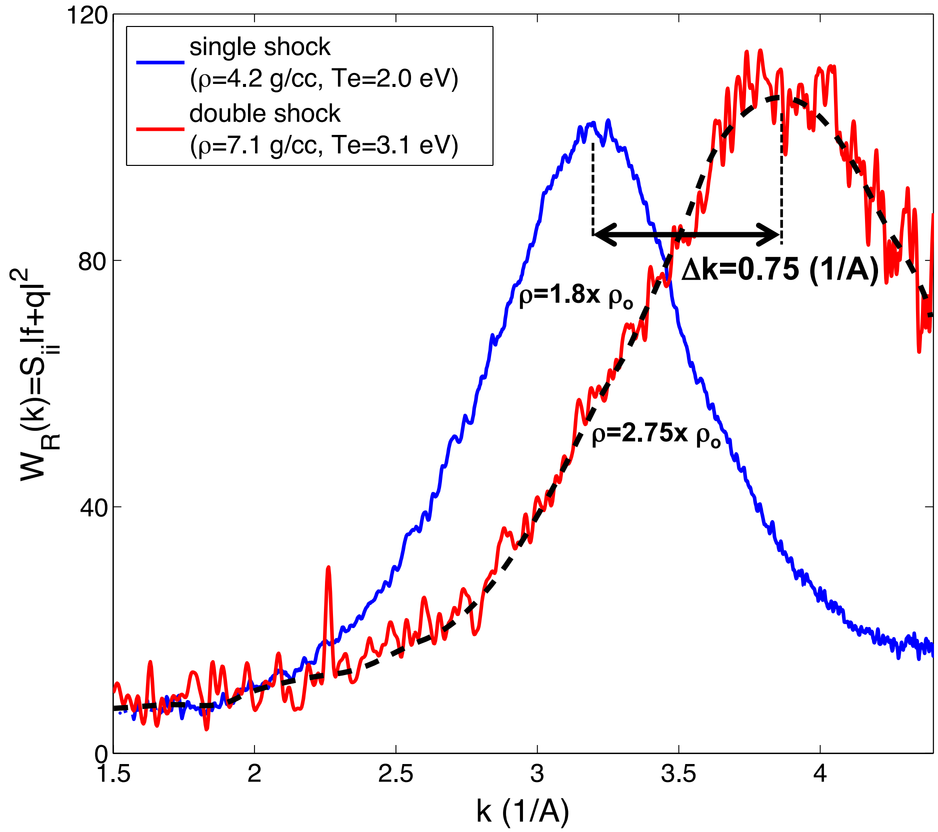

Continuous wavenumber resolved measurement

2 years versus 7 minutes

Measured ion-ion correlation peak

T. Ma *et al.*, *PRL 110, 065001 (2013)*

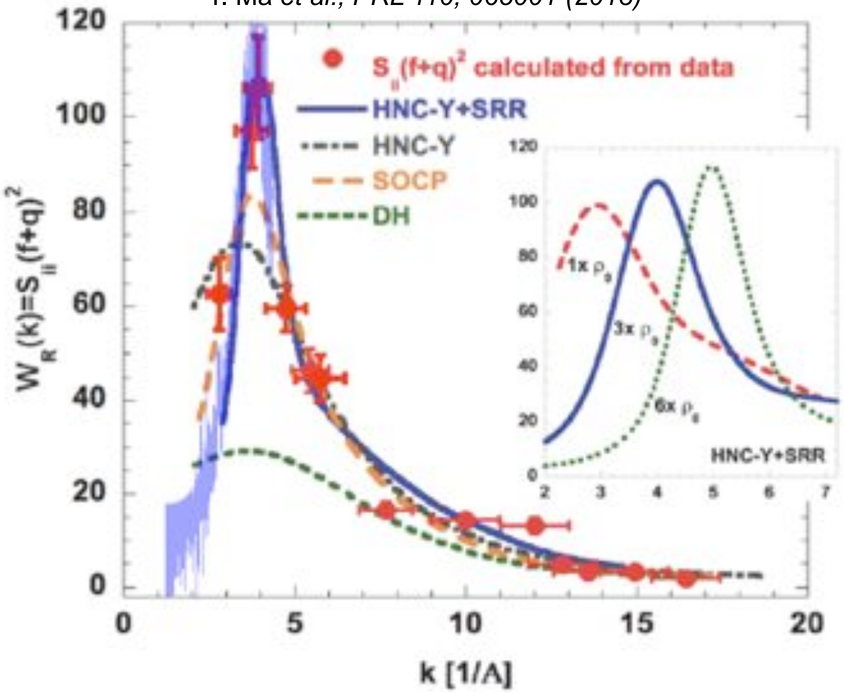

The shift and change in peak intensity of the correlation peak for 1.8x and 2.75x compressed aluminum, modeled using HNC-Y+SRR, can serve as a dynamic density diagnostic

Radial lineout (single shot)

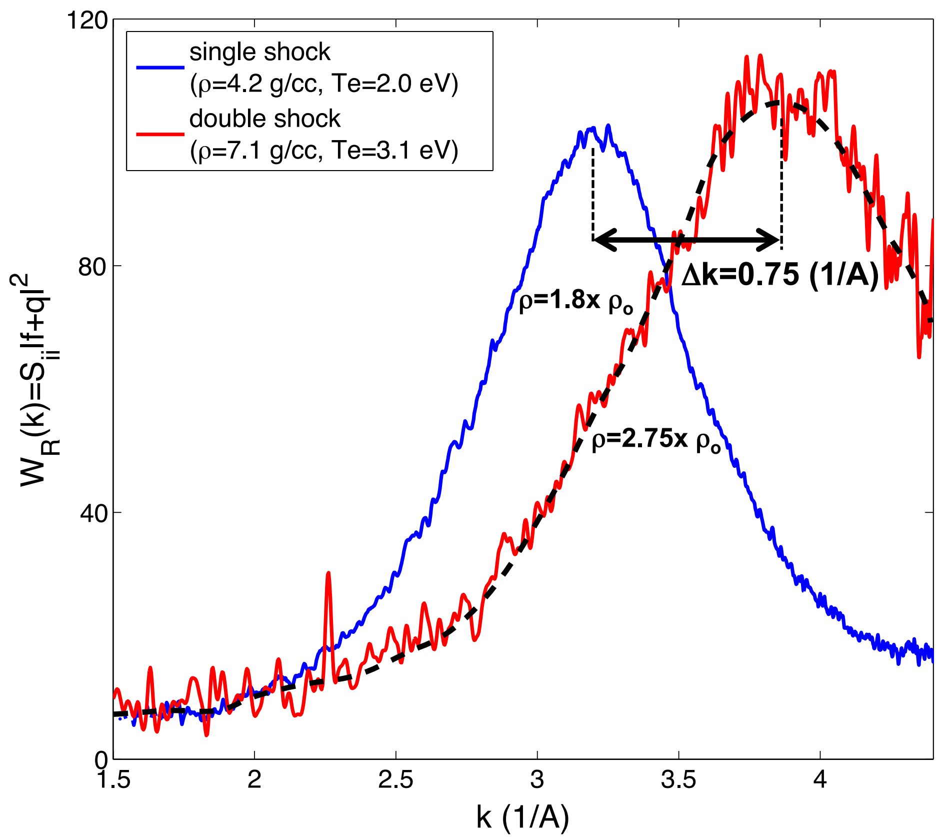

Continuous wavenumber resolved measurement

The ion-ion correlation peak has been measured in a number of shock-compressed samples

Aluminum

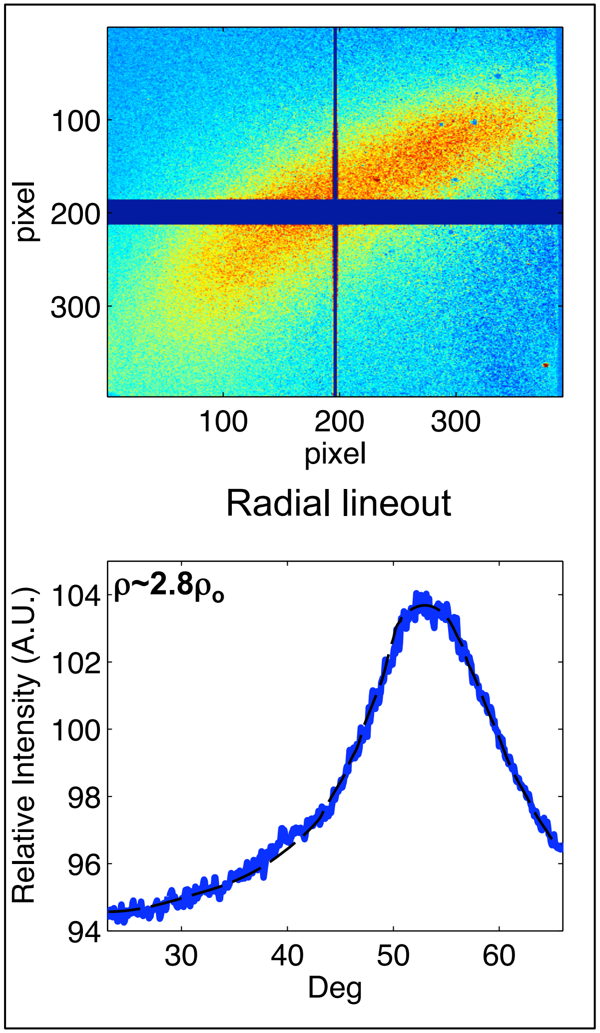

Magnesium

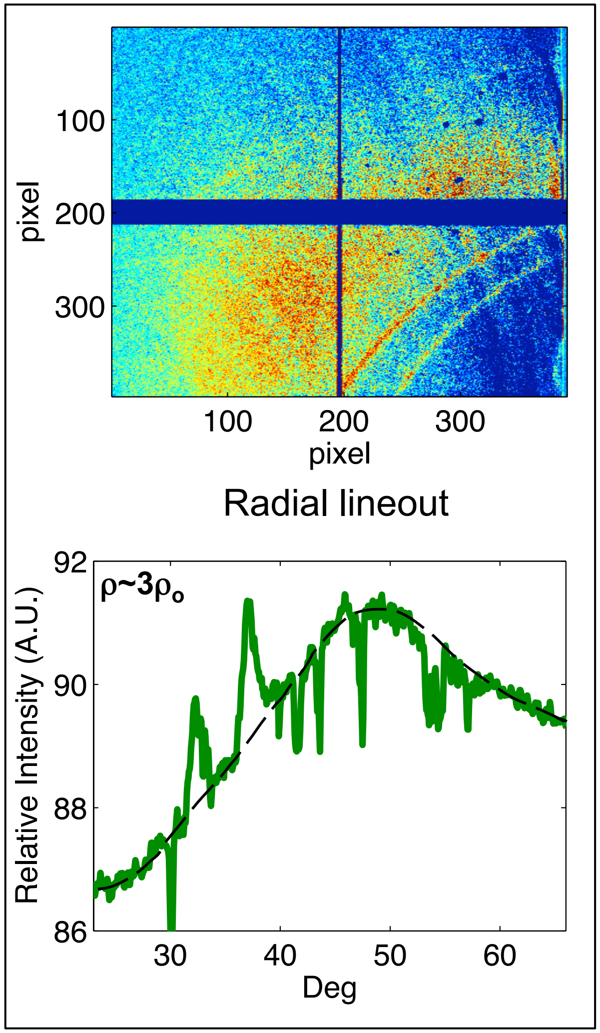

Carbon

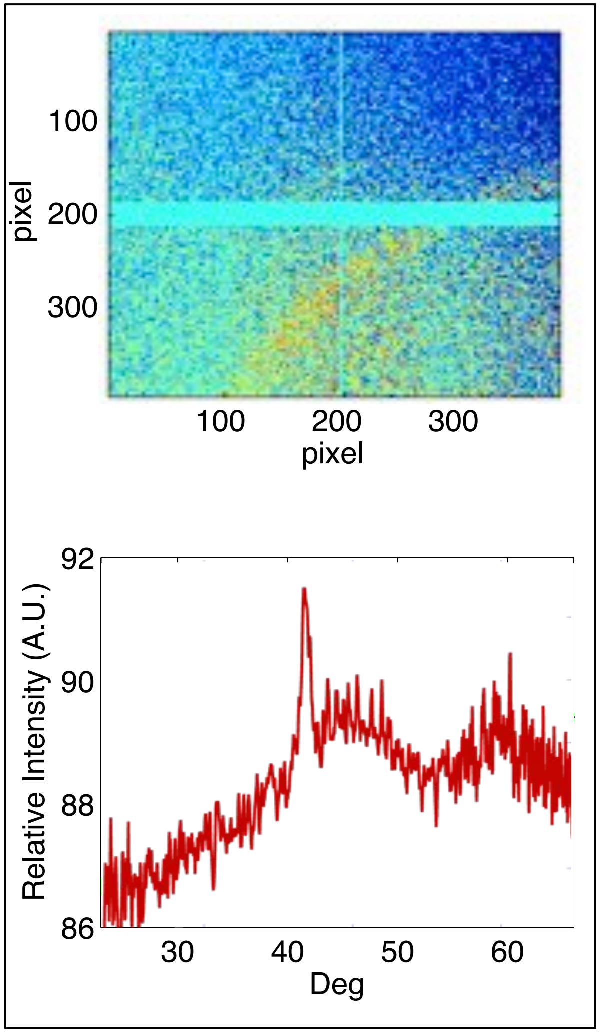

L. Fletcher et al., to be submitted

Workshop on high power lasers at SLAC

Home

High-Power Laser Workshop

SAVE THE DATE: October 1-2, 2013

SLAC National Accelerator Laboratory, Menlo Park, USA

This workshop will bring together the international science community to discuss the unique physics opportunities enabled by the new 200 TW laser at the Linac Coherent Light Source (LCLS). Coupling this laser to the world-class LCLS x-ray beam at the recently commissioned Matter in Extreme Condition (MEC) instrument will allow exquisite pump-probe experiments to address the most important physics questions of high-power laser plasma interactions physics in areas of high-energy density physics, laboratory astrophysics, laser-particle acceleration, and non-linear optical science.

The workshop will highlight recent results from MEC, describe the scientific opportunities for laser experiments at 200 TW and PW power and present and discuss the user access policy for performing laser experiments at MEC.

Hosts

Dr. Roger Falcone
Director of the Advanced Light Source, Lawrence Berkeley National Laboratory

Dr. Siegfried Glenzer
Distinguished Staff Scientist, SLAC National Accelerator Laboratory

Dr. Stefan Hau-Riege
Physicist, Lawrence Livermore National Laboratory

Sponsors – thank you

SLAC

- Support from DOE, Institutes, LCLS, company sponsors, and SLAC
  - Support 14 renowned speakers and discussion leaders
  - Support 19 students/postdoctoral scientists
- >140 scientists registered
  - 19 US university groups from 17 US universities
  - 8 US National laboratories
  - 11 US companies
  - 18 international groups from 9 countries

High-Power Laser workshop at SLAC, October 1st-2nd

SLAC

MEC user workshop on High-Power Lasers 2013

SLAC

19 US university groups
from 17 US universities

8 US National laboratories

11 US companies

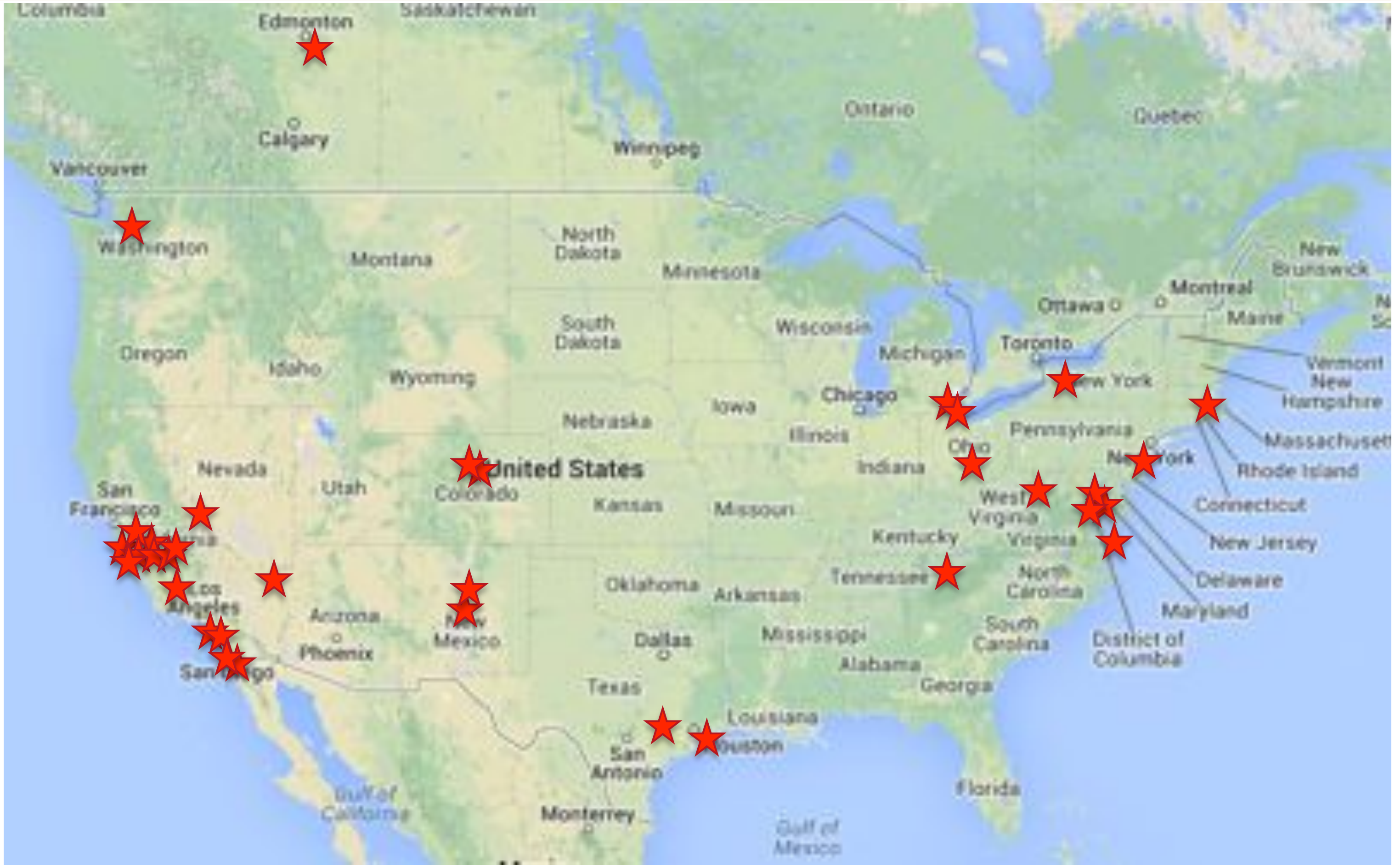

MEC user workshop on High-Power Lasers 2013

18 international groups from 10 different countries

Glenzer, FPA meeting, December 11, 2013

Goals for the workshop

SLAC

- To perform world-class HED physics at MEC/LCLS
- Need the input of the HED/HEDLP community
  - What are the important new directions in HEDLP?
  - How can we make best use of the unique combination of high-power lasers and LCLS x-rays?
  - What ideas need LCLS x-rays the most?
  - What new diagnostics and instrumentation is needed?

	High-Power Laser workshop schedule
Part I	**HED Physics at the MEC Instrument**
	Featured evening presentation
Part II	**Frontiers of High-Power Laser-Matter Interactions**
Part III	**High-Power Laser Science and Technology**
Part IV	**New Directions**
Part V	**MEC capabilities and priorities**
	Discussions

A new 200 TW-class laser will access important areas of Matter at Extreme Conditions

A high power laser will produce conditions important for HED physics, particle acceleration, and QED

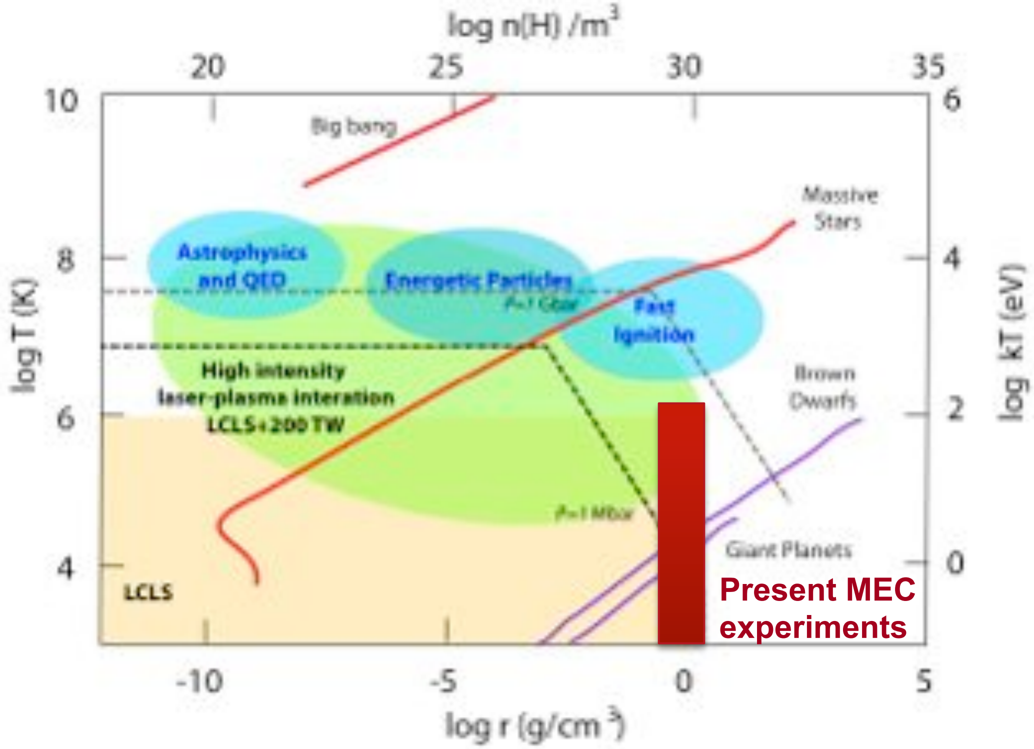

- Accurate probing of physics mechanisms will be accomplished by X-ray Thomson scattering with the LCLS beam
- Provides accurate temperature and density measurements
- Resolve micron scale length and fs time scales
- Determine laser coupling, heating, and pressure conditions

Path towards optimizing use of high-power petawatt lasers

Combining High-Power lasers with the world-class LCLS beam will allow novel experiments

Coupling of high-power lasers with matter	Physical properties of hot dense matter	Laboratory astrophysics

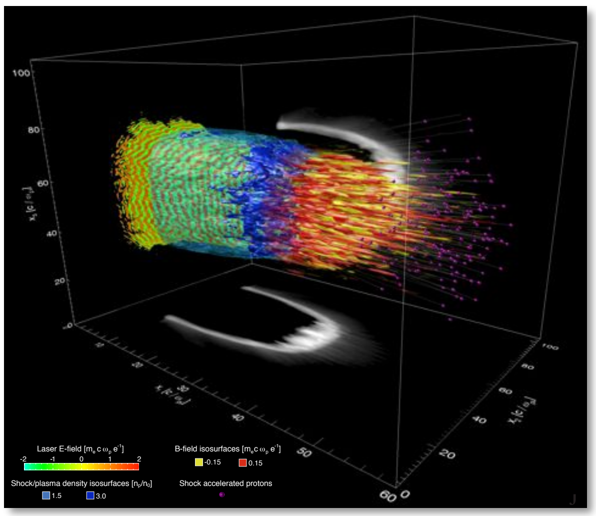

Fundamental laser-particle acceleration physics

- 100+ MeV protons
- Positrons
- Neutrons
- 10+ GeV electrons

X-ray Thomson scattering on hot dense matter matter

- Mbar pressures
- Isochorically heated matter
- Ultrafast phase transitions

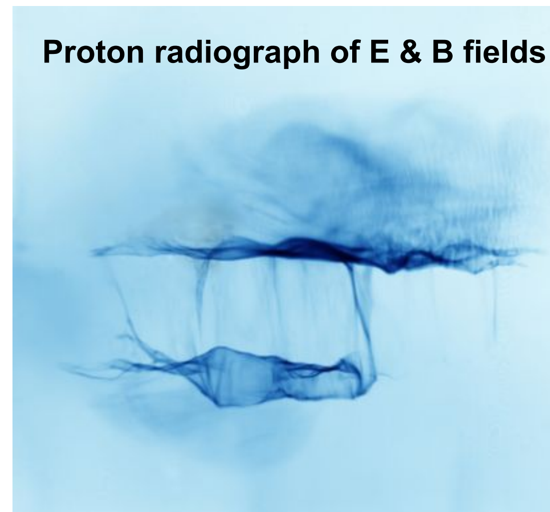

- Self organization in plasmas
- Weibel instabilities
- Collision less shocks
- Cosmic rays

Recent experiments have demonstrated a 200 TW laser driven betatron source

SLAC

The spectrometer provides both spectral and spatial information on the betatron source

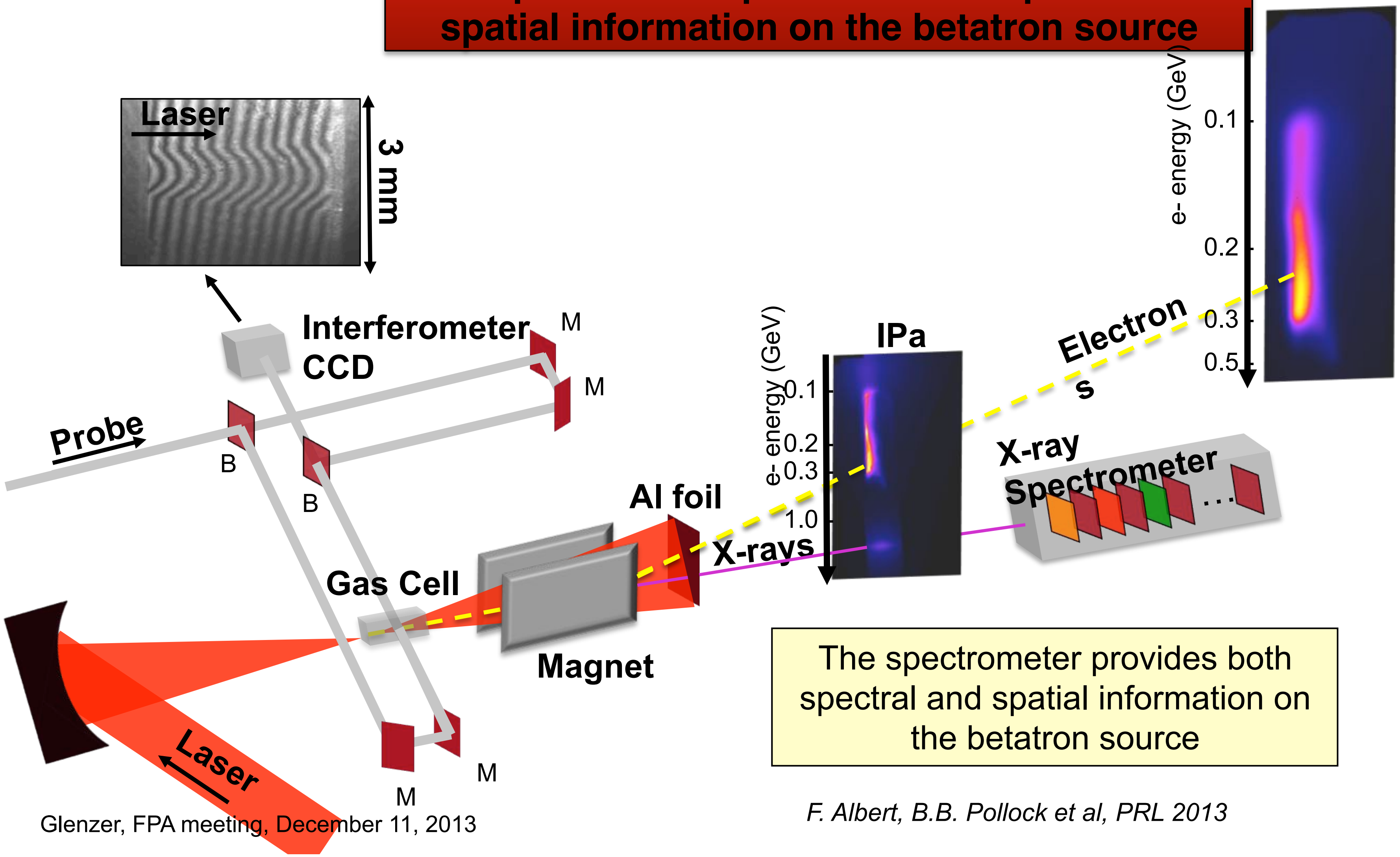

The spectrometer provides both spectral and spatial information on the betatron source

F. Albert, B.B. Pollock et al, PRL 2013

Laser-particle acceleration holds promise for new discoveries and applications

SLAC

Betatron x-rays from a 200 TW laser experiments provides 100 fs white light x-rays that scale to 100 keV for PW lasers

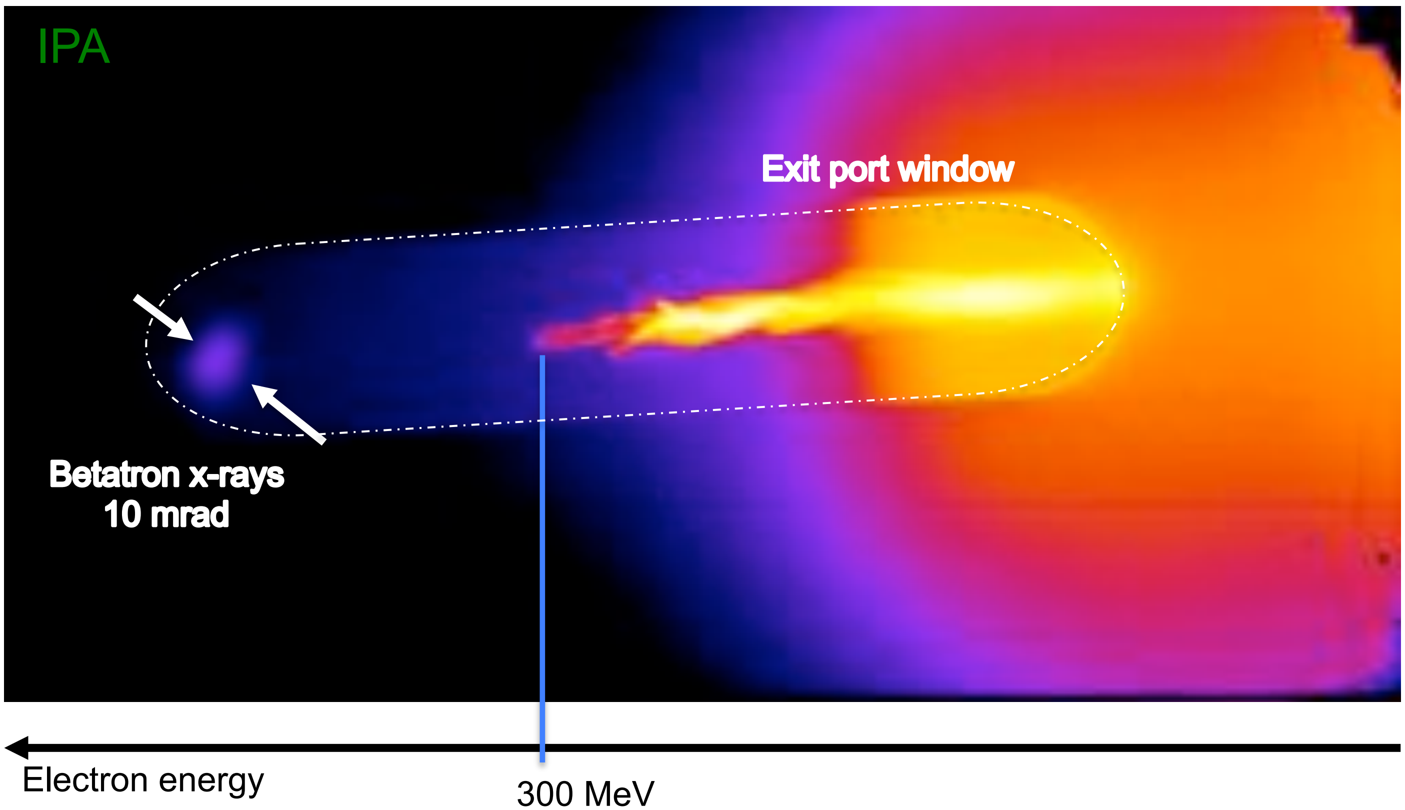

Multi-GeV electrons
Electron – x-ray interactions

- **F. Albert**
- **B. Pollock**

How does the peak brightness of a betatron x-ray source compare with other approaches?

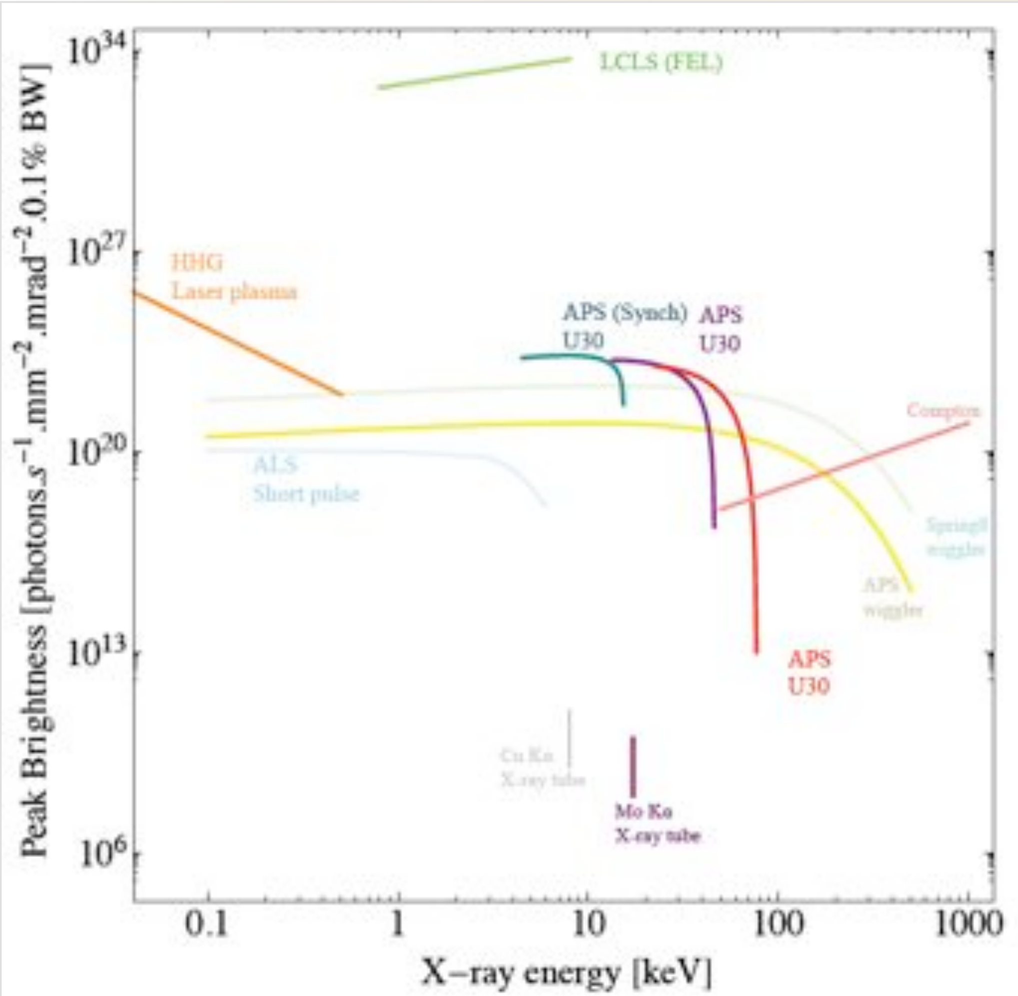

How does the peak brightness of a betatron x-ray source compare with other approaches?

SLAC

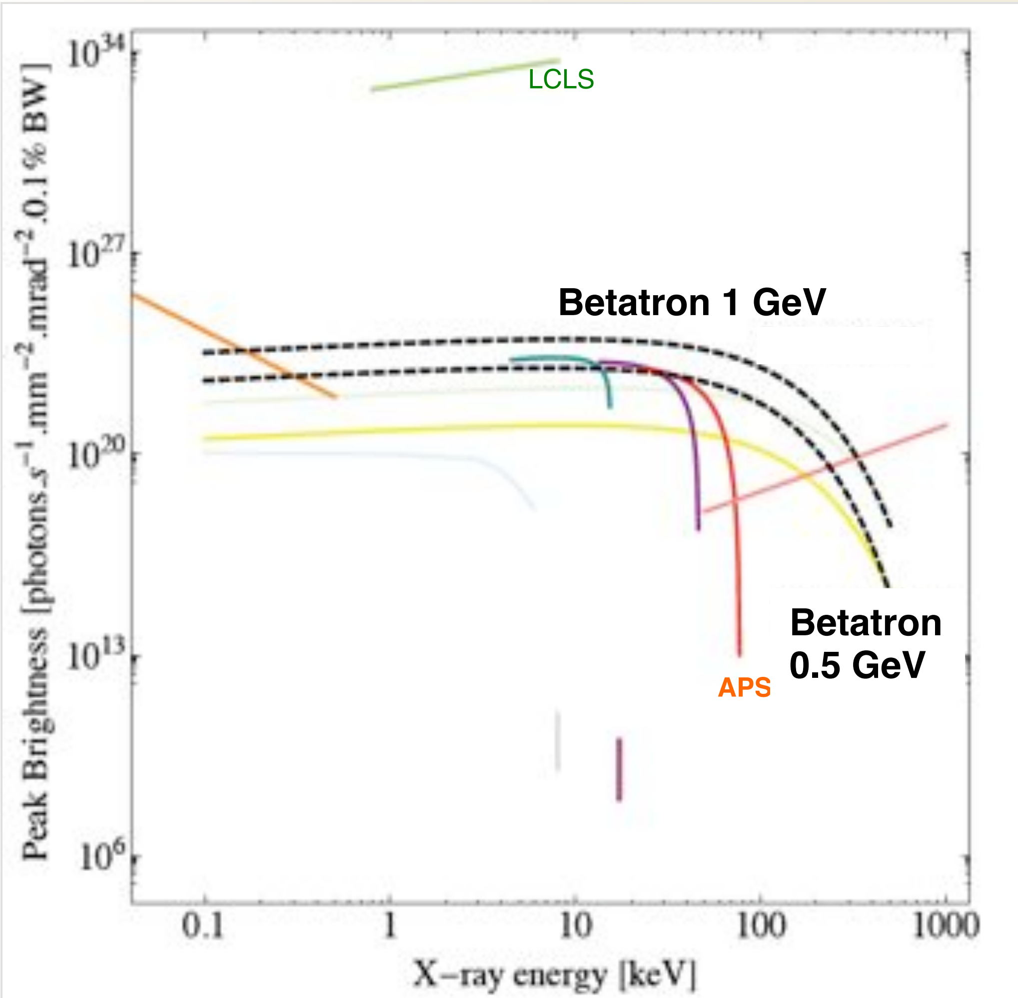

Parameter	Specification
Energy range	1-100 keV (broadband)
X-ray flux	10^8 photons/shot
Source size	1 micron
Source divergence	1-10 mrad (collimated)
Source duration	60 fs
Source maximum peak brightness	10^{22} photons/(mm^2 x mrad^2 x s. x 0.1 % BW)

Betratron radiator combine high brightness with high temporal resolution for x-ray x-ray pump probe experiments

Outline

- LCLS Free Electron Laser facility.
  - Unprecedented capabilities at the MEC instrument [since 4/2012]
    - 10^{12} x-ray photons for pump-prober experiments
    - High spectral resolution (seeded beam)
    - High wavenumber resolution (x-ray laser)
    - High temporal resolution (20-50 fs)
- Novel X-ray scattering experiments
  - First observation of Plasmon shift in shock-compressed plasmas
  - First continuous measurements of the dynamic structure factor
  - First observations of ion acoustic waves in warm dense plasmas
    - Pressures approaching 5-10 Mbar at 3x compressed Al
    - Test theoretical methods to determine pressures of dense matter
- Summary
    - High power laser workshop and outlook towards a bright future

We have a new precision tool to measure physical properties and to make transformative discoveries in High-Energy Density physics

End of Presentation

Discussion to combine LCLS with a PW laser
Example: 400J green will pump a 200 J, 200 fs laser

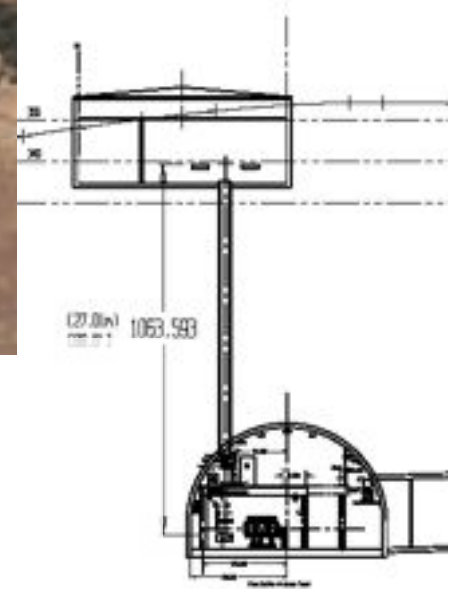

Example: Apollon laser footprint

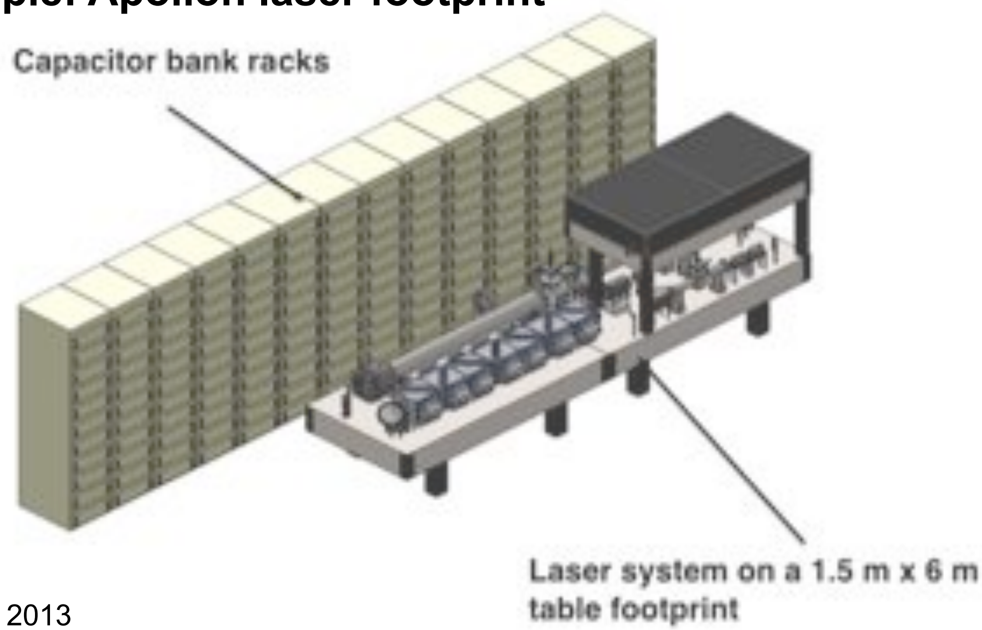

- 10 PW laser plans in Europe (ELI)
- HIBEF end station at XFEL (200 TW)
- SLAC: Need Building with shielding and infrastructure for PW
- High access option

These class of experiments have been initially proposed to DOE OFS

Shock compressed matter

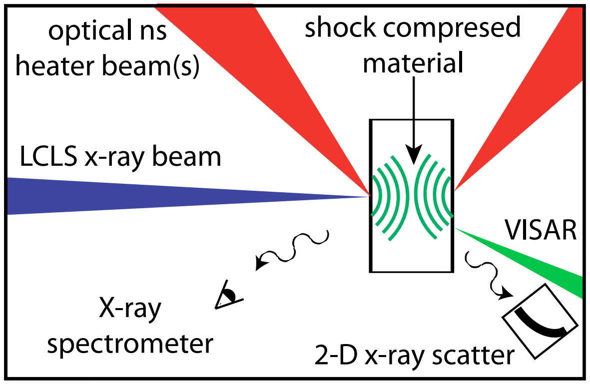

Ultrafast isochoric heating

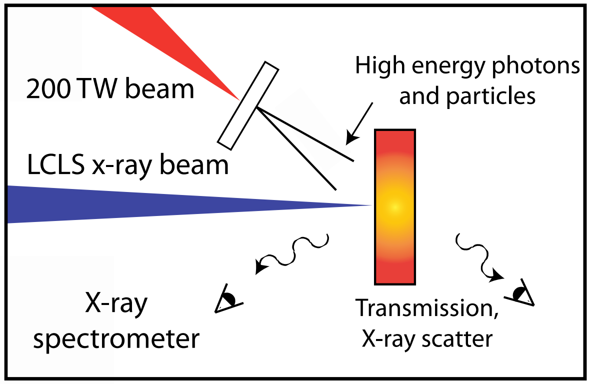

Relativistic plasmas

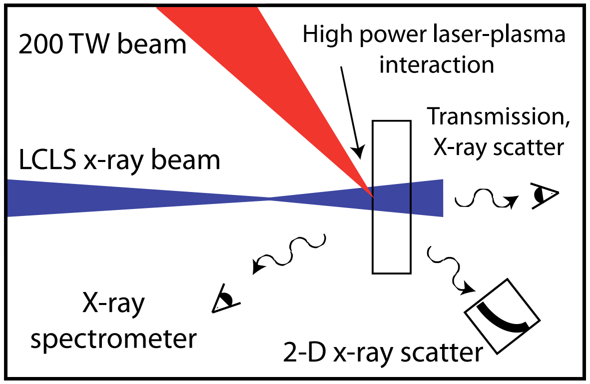

FORWARD proposal (Fundamental Optical Research With Advanced x-Ray Diagnostics)

Plasmon measurements accurately determine temperature and density

SLAC

Electron density variation:
n_e= 5.4 x 10^{23} cm^{-3} ± 10%

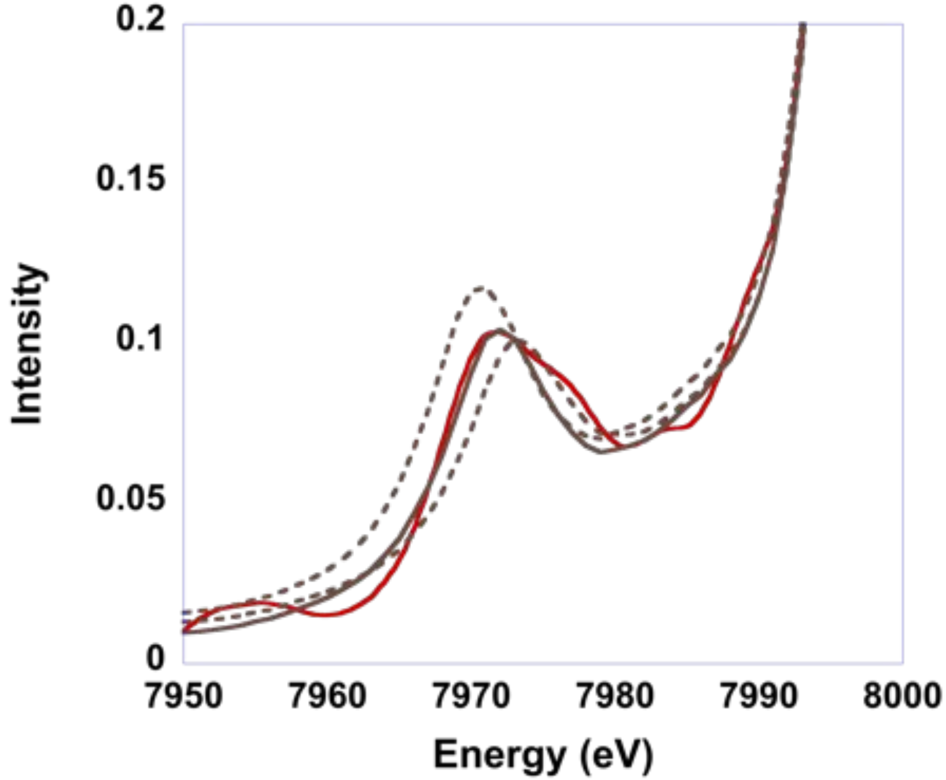

- Strong sensitivity to plasma frequency $\omega_{pe} = [n_e e^2/m_e \varepsilon_0]^{1/2}$

Ion temperature variation:
T_i= 3 eV ± 20%

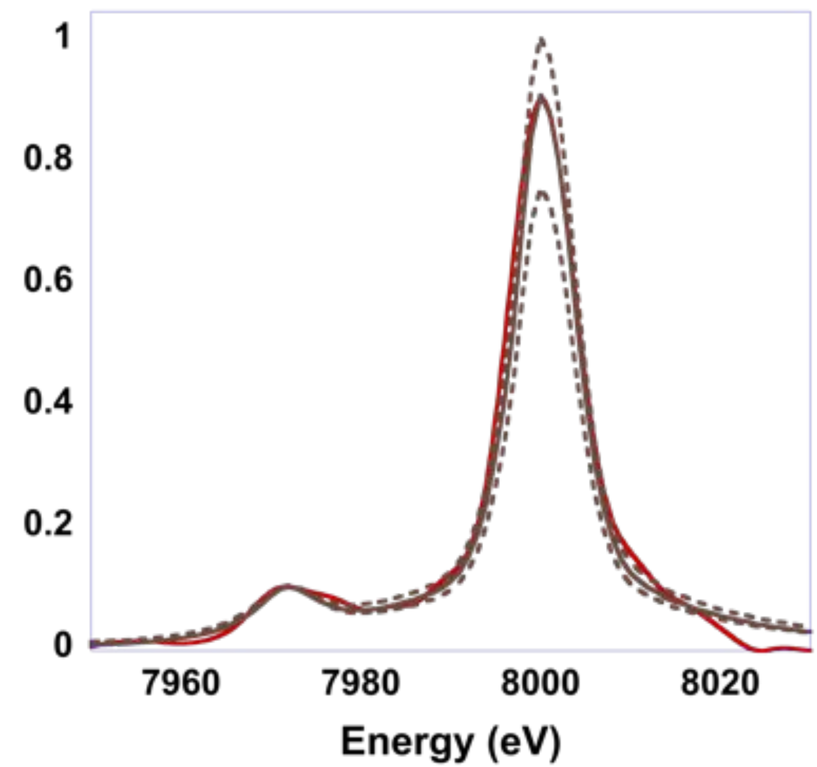

- Strong sensitivity to structure factor $S_{ii}(k)$

Wavenumber resolved scattering data indicate negative screening

SLAC

Using short range repulsion provides an excellent fit to W(k)

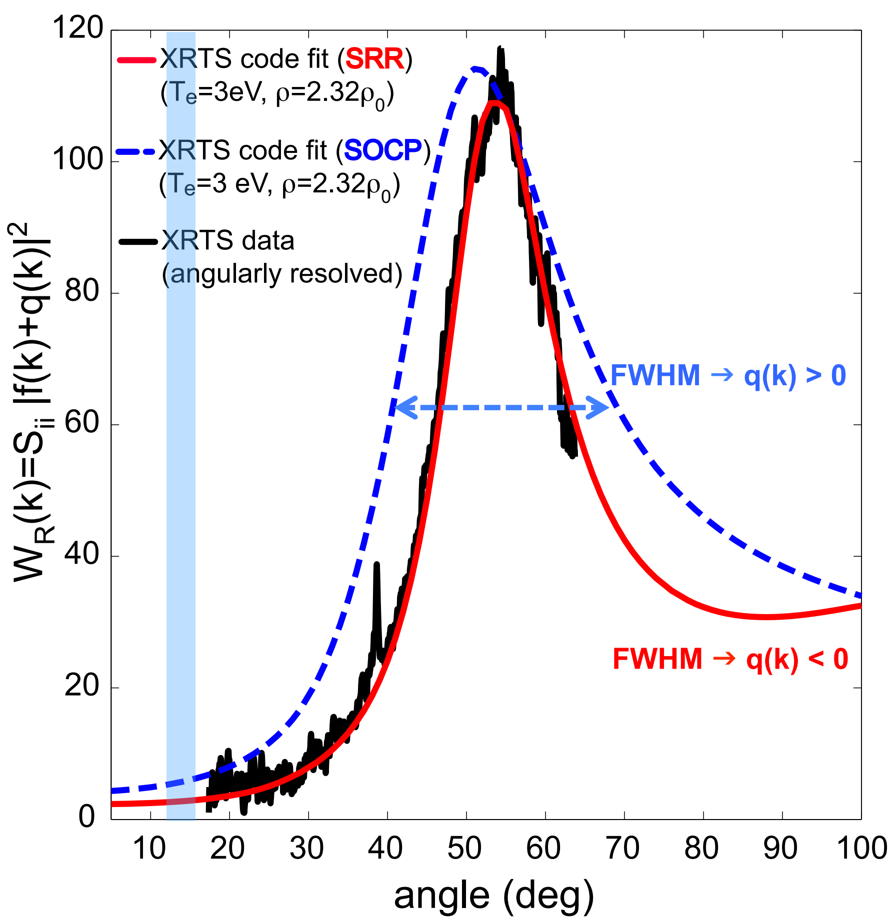

Using short range repulsion provides an excellent fit

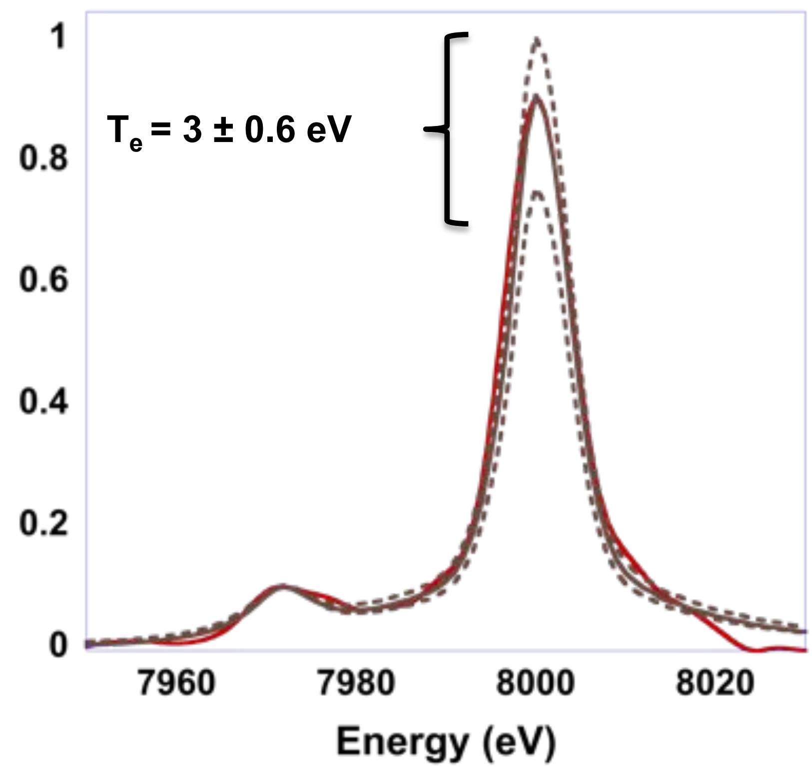

The measured densities from plasmon data yields a critical experimental test of the ion structure factor, where a strong sensitivity also provides an accurate temperature measurement

LCLS experiments of the microphysics have provided new insights in ICF ablator physics

SLAC

- X-ray Thomson scattering experiments at Omega have shown densities of $n_e = 10^{24} cm^{-3}$ a factor of 2 higher than standard radiation-hydrodynamic simulations with a Thomas-Fermi model
- Using improved continuum lowering models tested in LCLS experiments (Stewart-Pyatt, Ecker-Kröll) provide excellent agreement
- The conditions emulate ICF capsule ablator conditions during ICF implosions - accurate modeling of these plasmas is important to calculate hydrodynamic instabilities and compression

X-ray Thomson scattering measurements of highly compressed CH at 50 Mbar ICF conditions (Fletcher et al.)

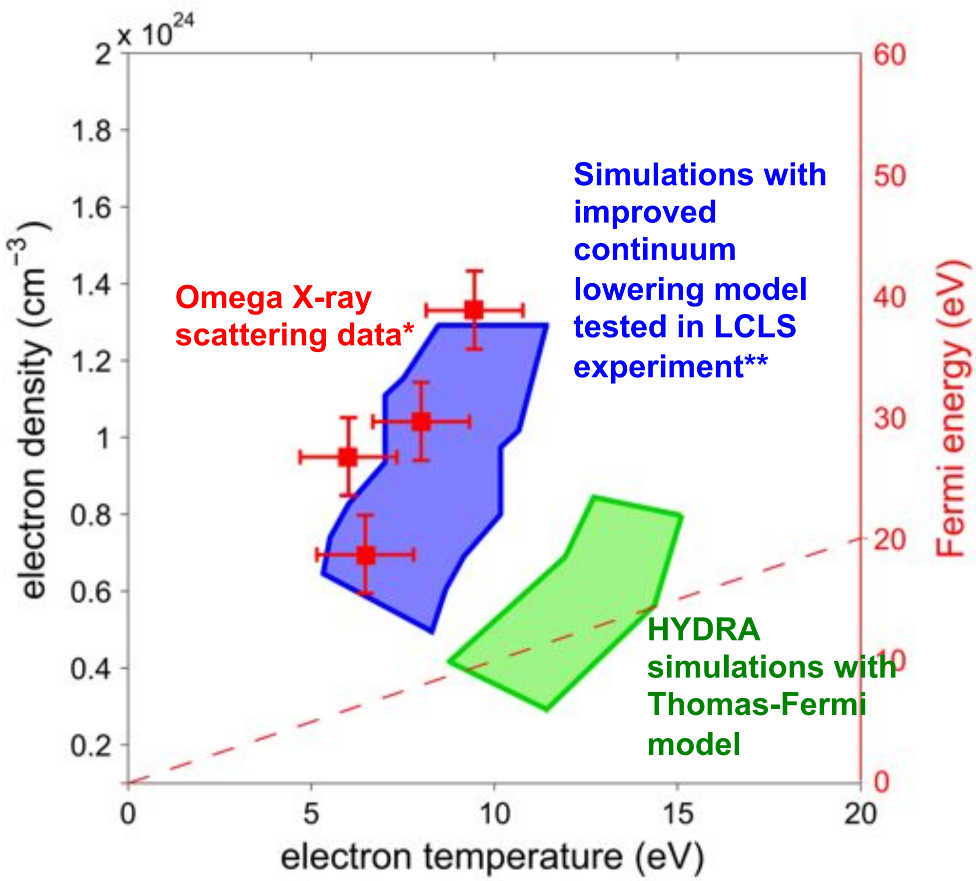

- A.L. Kritcher et al., PRL 107, 015002 (2011),
- L. Fletcher, Phys. Plasmas (2013), in print

** O. Ciricosta et al., PRL 109, 065002 (2012)

Laser-particle acceleration holds promise for new discoveries and applications

Laser wakefield >1 GeV acceleration of electrons	Laser proton and He+ acceleration to >100 MeV	Neutron beams >2 e9 neutrons

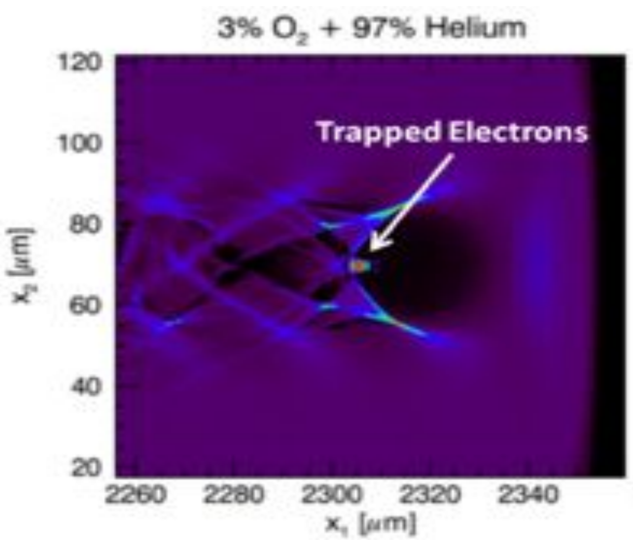

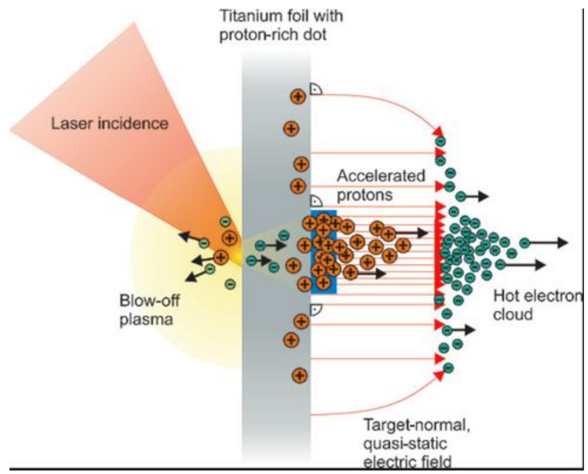

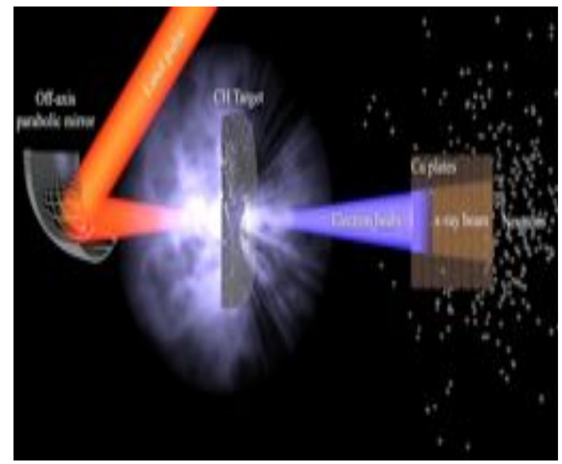

Multi-GeV electrons
Electron – x-ray interactions
Isochoric heating
Record magnetic fields

- **K. Krushelnik**
- **B. Pollock**
- **T. Tajima**
- **C. Haefner**

Isochoric heating of matter
Equation of state of warm dense matter
Medical applications

- **T. Ditmire**
- **M. Hegelich**
- **M. Roth**
- **G. Korn**
- **G. Mourou**

Fusion processes
Fusion diagnostics and target chambers
Material science

- **E. Moses**
- **D. Froula**
- **P. Chen**
- **J. Wark**

Plasmas produced with high-intensity lasers accelerate and wiggle electrons to emit Betatron x-rays

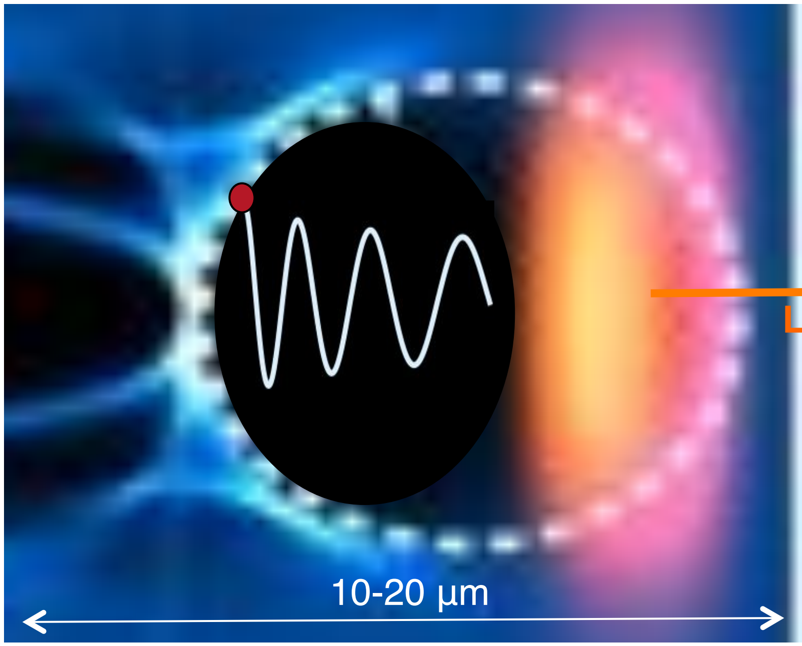

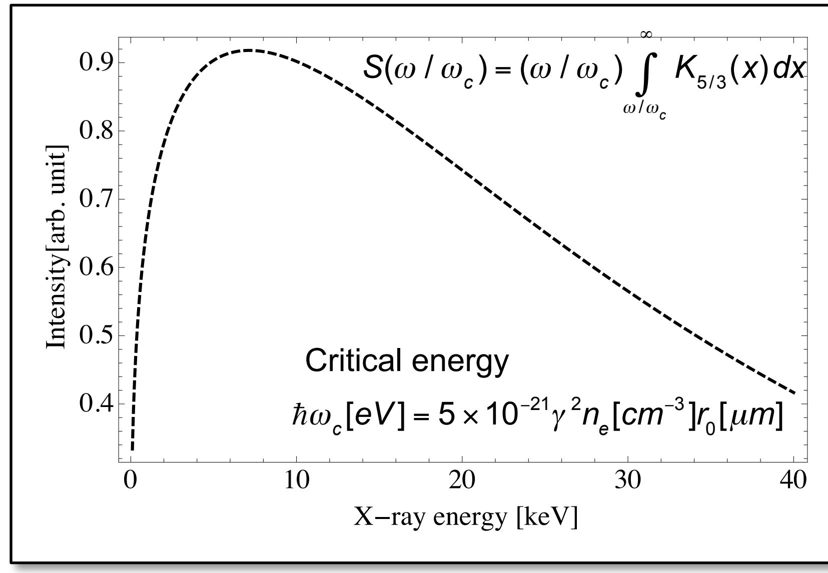

To obtain ~ 25 keV Betatron X-rays we need:

High energy electrons ($\gamma>1000$ or $E>0.5$ GeV)

Electron densities 10^{18}-10^{19} cm^{-3}

Oscillations amplitude 1-5 μm

Novel particle acceleration mechanism based on Weibel instability from high power laser-driven currents

Laser:
$I_{Laser} = 10^{20}$-10^{21}W cm^{-2}
Target
$n_e=10^{22}$-10^{23} cm^{-3}

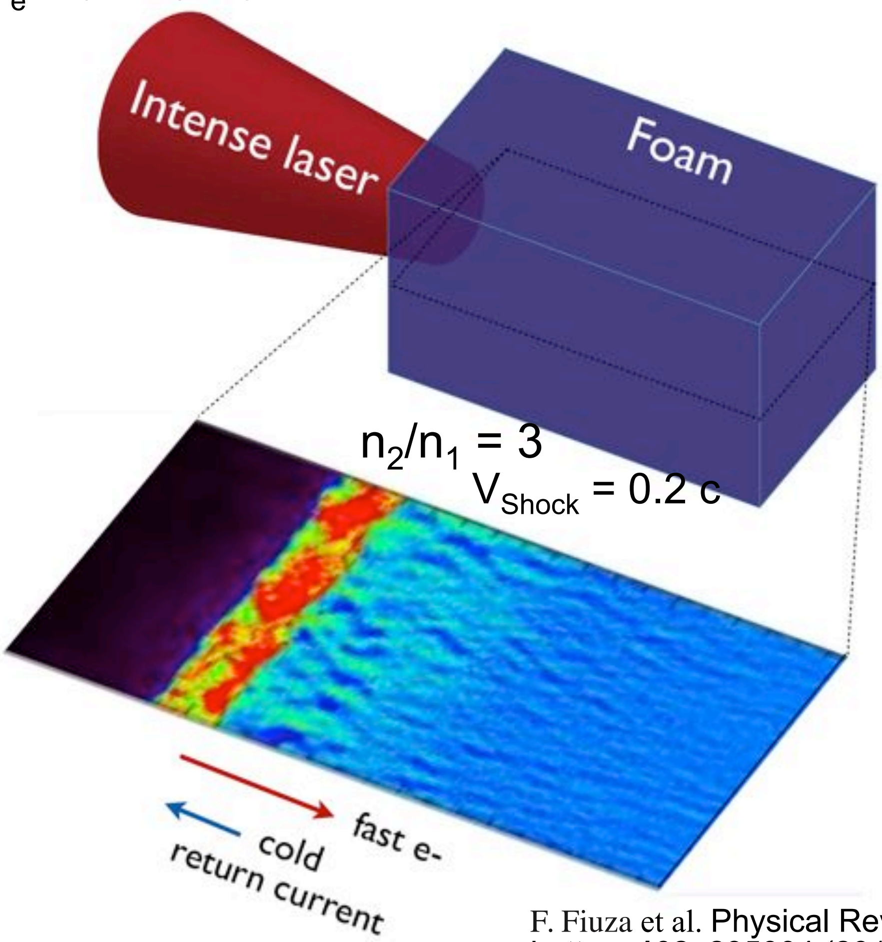

F. Fiuza et al. Physical Review Letters **108**, 235004 (2012).

Counter propagating currents: B-field growth by Weibel instability

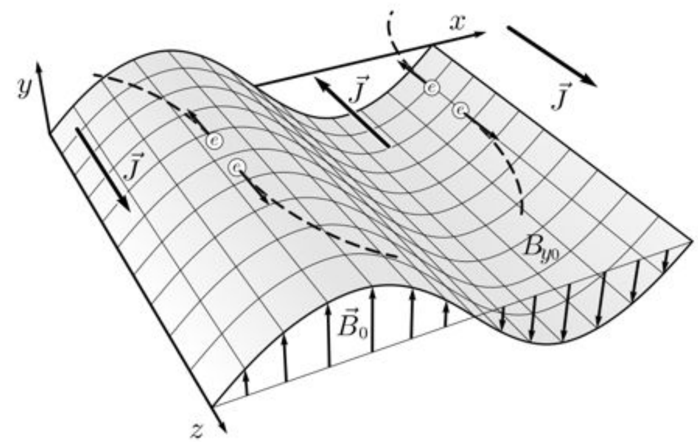

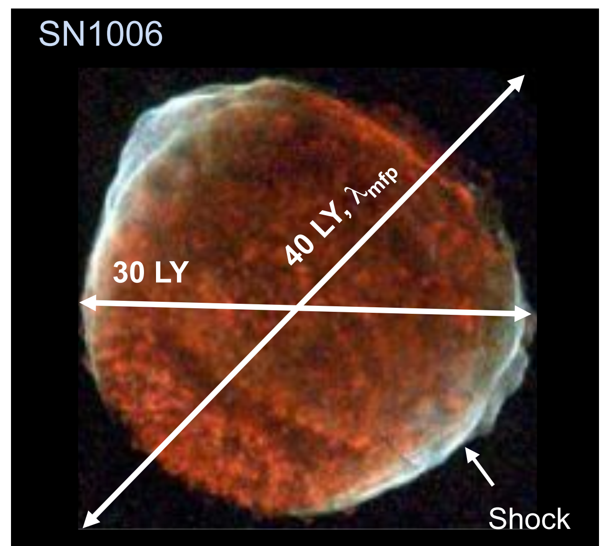

A fully developed Weibel mediated collision-less shock can be driven by a high laser power

SLAC

30 – 200 TW, 5 – 0.01 Hz; Scheduled: Q2, FY14

t (fs)	P (TW)	w_0 (mm)	a_0	n_p/n_{cr}	β_{sh}
200	35	5	5.7	6	-
400	17.5	5	4	5	-

Peta watt laser conditions

t (fs)	P (TW)	w_0 (mm)	a_0	n_p/n_{cr}	β_{sh}
400	1750	5	23	50	0.05
800	875	5	16	35	0.04

Weibel instability

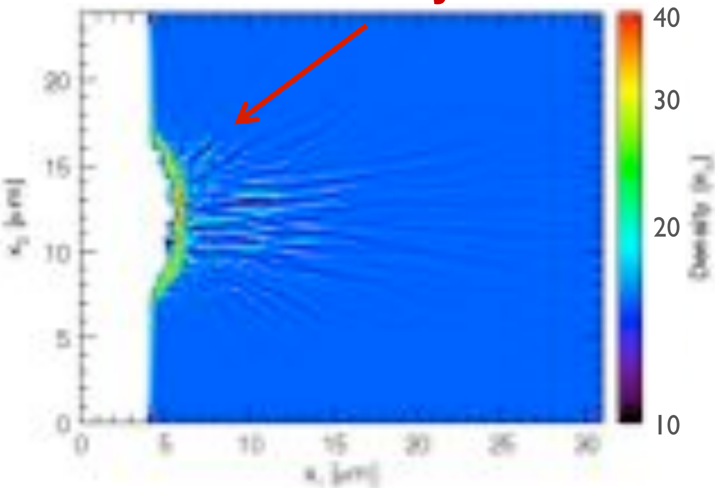

Fully developed shock

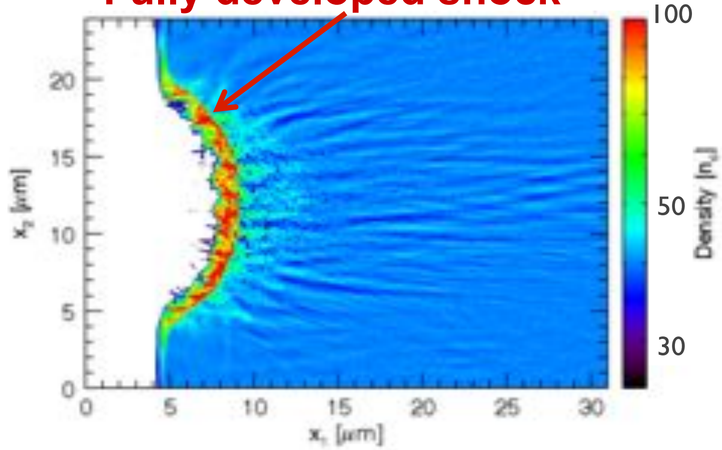

*Calculations with PIC code OSIRIS, F. Fiuza

Simulations predict observations of high energy particles at PW laser power